



140  
538  
THS



**PLACE IN RETURN BOX** to remove this checkout from your record.  
**TO AVOID FINES** return on or before date due.  
**MAY BE RECALLED** with earlier due date if requested.

<b>DATE DUE</b>	<b>DATE DUE</b>	<b>DATE DUE</b>

**SEPARATION AND QUANTITATION OF NITRATED EXPLOSIVES USING  
THIN-LAYER CHROMATOGRAPHY AND CHARGE-COUPLED DEVICE  
CAMERA IMAGING**

**By**

**Melissa Sue Meaney**

**A THESIS**

**Submitted to  
Michigan State University  
in partial fulfillment of the requirements  
for the degree of**

**MASTER OF SCIENCE**

**School of Criminal Justice**

**2007**

## **ABSTRACT**

### **SEPARATION AND QUANTITATION OF NITRATED EXPLOSIVES USING THIN-LAYER CHROMATOGRAPHY AND CHARGE-COUPLED DEVICE CAMERA IMAGING**

By

Melissa Sue Meaney

In recent years, the analysis of nitrated explosives has become increasingly important in the forensic community. In cases of national security or on the front lines of international conflicts, sophisticated technologies for explosives detection are available and widely used. For less prominent cases, however, state and local law enforcement and forensic laboratories are not equipped with such state-of-the-art, field-ready equipment. One of the most common preliminary screening techniques used in these situations is thin-layer chromatography (TLC) with spray reagents, followed by identification by visual inspection. This project has sought to improve the TLC separation of nitrated explosives using less toxic solvents to decrease safety concerns while maintaining the inherent simplicity. An analysis procedure was identified to separate an unknown explosive sample containing up to 12 explosives in two steps. In addition, fluorescence imaging has been utilized for quantitation of nitrated explosives and degradation products following TLC separation. Explosives were quantitated over three orders of magnitude with practical detection limits in the low microgram range. This method is appealing because it can be performed with commonly-used equipment such as a handheld UV light source and a digital camera.

**To My Friends and Family, and To Andrew, with Love**

## **ACKNOWLEDGEMENTS**

For my start in forensic science, I must thank my father. Without his fascination with criminal dramas and Court TV in the late 1990s (before they were popular), I would have never been inspired toward this great career path. From there, I thank Dr. Jay Siegel for accepting me into the prestigious forensic science program at Michigan State University, and staying with me through this process although his own career took him to Indiana University-Purdue University Indianapolis. He has been a great mentor and my best resource for all knowledge that is forensic science. It was also Jay who encouraged me to pursue a Ph.D. in chemistry, and without his unbelievable insight, I would not be where I am today.

I must also give many thanks to my other advisors at Michigan State University, Dr. Victoria McGuffin and Dr. Ruth Waddell Smith, for their continued support. Vicki helped guide this research project from beginning to end, and insisted that it continue despite many setbacks. Her knowledge of separation science and spectroscopy, in addition to a vast amount of practical expertise, are directly reflected in the content and structure of this work. Although Ruth arrived after much of this research was completed, she was willing to handle much of the editing aspects of the thesis. Ruth was also invaluable in providing feedback and suggestions to improve both my research and my writing. I was also blessed with two excellent women role models, both of whom are incredibly successful and more than willing to share their knowledge and experience. I would also like to thank Dr. Mahesh Nalla for his willingness to provide feedback as a member of

my thesis committee. In addition, I would like to thank Dr. David Foran and Chris Bommarito of the Michigan State Police for teaching me so much about forensic biology and practical forensic chemistry, respectively.

I was fortunate enough to work with Jenny Borowitz, an amazing undergraduate student, on this work. Jenny worked diligently for nearly a year to complete many of the separations and acquire much of the data that is presented in this work. As a senior B.S. Chemistry major, she managed to fit undergraduate research into her already overloaded schedule. Jenny's ideas and creativity helped us overcome a number of hurdles during this research project, and her enthusiasm and dedication are what made this project so enjoyable. I am greatly appreciative of her hard work and truly indebted to her for the time she spent working with me. I also want to thank my good friend Amber Hupp for her help with the final parts of this research project by preparing blind samples for the validation of the methods.

Lastly, I must thank my friends and family who have supported me through my time in graduate school. Thanks to Elizabeth, Carl, and Audrey for sharing in the experience of a dual degree program and all of the headaches that entails. Thanks to Sam, Carl, Xiaoping, Rashad, Amber, Kahsay, Heidi, Lucas, John, and Melissa for being the best group members a girl could ask for. Thanks to Elizabeth, Amber, Audrey, Anne, Jason, Alli, Lucas, Dan, and Lisa for being great friends, and knowing when it's about work and when it's not. Thanks to Lucas, Lisa, and Sarah for being a fun bunch and inviting me to Tuesday lunch. Thanks to Erin, Sarah, Kristin, and Lisa, my friends outside of chemistry and

forensic science, for keeping me grounded. Thanks to my softball team for keeping me active and sharing lots of good memories on and off the field. Thanks to Mom, Dad, Melinda, Jerrod, Matt, Stephanie, Gerri, Don, Geoff, Donna, and Kevin for their willingness to accept my absence at many family events and for their unquestionable joy when I was in attendance. A special thank you to my parents for always believing in me and encouraging me to pursue my goals and dreams. Thanks to my nieces and nephews who just love their Aunt Mel. Lastly, thanks to Andrew, for being by my side unconditionally through this process that you don't understand. We have been on an amazing journey through these past few years, and I can't wait for it to continue as I spend the rest of my life with you.

## TABLE OF CONTENTS

<b>LIST OF TABLES .....</b>	<b>ix</b>
<b>LIST OF FIGURES.....</b>	<b>xi</b>
<b>KEY TO ABBREVIATIONS.....</b>	<b>xiv</b>
<b>CHAPTER 1. INTRODUCTION.....</b>	<b>1</b>
1.1 Explosives.....	2
1.2 Explosives as Evidence .....	8
1.3 Established Methodologies .....	9
1.4 Thin-Layer Chromatographic Analysis of Explosives .....	11
1.5 Detection of Explosives Following Thin-Layer Chromatography .....	12
1.6 Research Objectives.....	15
1.7 References .....	16
<b>CHAPTER 2. SEPARATION OF NITRATED EXPLOSIVES .....</b>	<b>21</b>
2.1 Experimental Methods .....	21
2.1.1 Chemicals .....	21
2.1.2 Plate Preparation .....	22
2.1.3 Plate Development .....	23
2.2 Theory of Adsorption Chromatography .....	24
2.3 Separation of TNT and Degradation Products .....	30
2.4 Separation of Nitroaromatic Explosives .....	35
2.5 Separation of Nitroaromatic and Nitrate Ester Explosives .....	36
2.6 Separation of Nitramine Explosives .....	39
2.7 Precision of Retention Factors.....	40
2.8 Separation of an Unknown Explosive Sample .....	43
2.9 Conclusions .....	46
2.10 References .....	47
<b>CHAPTER 3. QUANTITATION OF NITRATED EXPLOSIVES.....</b>	<b>48</b>
3.1 Positioning of Imaging System Components .....	48
3.2 Optimization of Image Acquisition and Manipulation .....	50
3.3 Correction Using a Background Plate .....	57
3.4 Theory and Data Analysis.....	59
3.5 Quantitation of Degradation Products.....	63
3.6 Quantitation of Nitroaromatic Explosives .....	72
3.7 Quantitation of Nitramine Explosives .....	76
3.8 Quantitation of Nitrate Ester Explosives.....	79
3.9 Quantitation of an Unknown Explosive Sample .....	82
3.10 Additional Observations .....	85

3.11	Conclusions .....	86
3.12	References .....	87
<b>CHAPTER 4. CONCLUSIONS AND FUTURE DIRECTIONS.....</b>		<b>88</b>

## LIST OF TABLES

Table 1.1	Explosives and degradation products used to validate TLC separation and CCD imaging system.....	3
Table 1.2	Common military explosives and formulations. ....	7
Table 2.1	Group adsorption energies for substituents common to nitrated explosives and degradation products.....	26
Table 2.2	Net adsorption energies for explosives and degradation products	28
Table 2.3	Properties of common TLC mobile phases .....	31
Table 2.4	The precision of retention factors for nitroaromatic explosives and degradation products in 88:12 hexane:THF. ....	34
Table 2.5	The precision of retention factors for nitroaromatic explosives in 70:30 cyclohexane:MEK. ....	37
Table 2.6	The precision of retention factors for nitroaromatic and nitrate ester explosives in 88:12 hexane:THF. ....	38
Table 2.7	The precision of retention factors for nitramine explosives in 50:50 hexane:THF. ....	41
Table 2.8	The precision of retention factors for nitramine explosives and picric acid in 65:35 hexane:MEK .....	42
Table 2.9	Analysis of unknown explosive sample 1. ....	44
Table 2.10	Analysis of unknown explosive sample 2. ....	45
Table 3.1	Comparison of image quality for various gain settings obtained with an integration time of 500 ms.....	54
Table 3.2	Comparison of image quality for various integration times.....	56
Table 3.3	Comparison of image quality for summing and averaging pixels in different size selections of the image .....	58
Table 3.4	Detection figures of merit for nitrated explosives and degradation products using the semi-logarithmic function (Equation 3.4).....	69
Table 3.5	Detection figures of merit for nitrated explosives and degradation products using the logarithmic function (Equation 3.5).....	70

Table 3.6	Analysis of unknown explosive samples. ....	84
-----------	---	----

## LIST OF FIGURES

- Figure 1.1 Common nitroaromatic explosives: (1) TNT, (2) picric acid, and (3) Tetryl. Nitramine explosives: (3) Tetryl, (4) RDX, and (5) HMX. Nitrate ester explosives: (6) NG and (7) PETN. .... 5
- Figure 1.2. Some common degradation products of TNT used in this work: (8) NB, (9) 2-NT, (10) 2,4-DNT, (11) 2,6-DNT, and (12) 4-am-DNT. .... 6
- Figure 2.1 Sample plate containing (I) a reference sample and (II) an unknown sample. Designated plate areas include (a) the original location and a completely retained solute ( $R_f = 0$ ), (b) the solvent front, (c,e) a solute ( $R_f(c) = 0.21$ ,  $R_f(e) = 0.66$ ) that is detected in the reference sample but undetected in the unknown sample, (d) a solute ( $R_f = 0.56$ ) that is detected in both the reference and unknown samples at similar concentrations, and (f) a solute ( $R_f = 0.87$ ) that is detected at a higher concentration in the reference sample than in the unknown sample... .. 25
- Figure 2.2 Effect of percent THF in hexane on the retention factors measured for TNT (■) and degradation products, including NB (○), 2-NT (●), 2,4-DNT (◆), 2,6-DNT (□), and 4-am-2,6-DNT (◇). .... 33
- Figure 3.1. Diagram of TLC plate imaging setup..... 49
- Figure 3.2 Fluorescence of a TLC plate at various times after turning on the UV lamp: (a) 5 min, (b) 15 min, (c) 25 min, (d) 35 min, (e) 45 min, (f) 55 min, (g) 65 min..... 51
- Figure 3.3 Simulated images and chromatograms for (1) a background plate and (2) a sample plate containing (I) a reference sample and (II) an unknown sample. Designated plate areas include (a) the original location and a completely retained solute, (b) the binning area around a strongly retained solute that is undetected in the unknown sample and the corresponding chromatogram, (c) the binning area around a weakly retained solute detected in both samples but at different concentrations and the corresponding chromatogram, and (d) the solvent front. The corrected intensity is calculated by using Equation 3.1..... 53
- Figure 3.4. Fit of TNT to the symmetric double-sigmoidal function (Equation 3.3). (A) Corrected intensity for 9.8  $\mu\text{g}$  TNT. (B) Symmetric double-sigmoidal fit of 9.8  $\mu\text{g}$  TNT data (— — —),  $R^2 = 0.987$  ..... 61

Figure 3.5	Calibration curves for NB based on peak area using (A) the semi-logarithmic fit described in Equation 3.4 and (B) the logarithmic fit described in Equation 3.5.....	64
Figure 3.6	Calibration curves for 2-NT based on peak area using (A) the semi-logarithmic fit described in Equation 3.4 and (B) the logarithmic fit described in Equation 3.5.....	65
Figure 3.7	Calibration curves for 2,4-DNT based on peak area using (A) the semi-logarithmic fit described in Equation 3.4 and (B) the logarithmic fit described in Equation 3.5.....	66
Figure 3.8	Calibration curves for 2,6-DNT based on peak area using (A) the semi-logarithmic fit described in Equation 3.4 and (B) the logarithmic fit described in Equation 3.5.....	67
Figure 3.9	Calibration curves for 4-am-DNT based on peak area using (A) the semi-logarithmic fit described in Equation 3.4 and (B) the logarithmic fit described in Equation 3.5.....	68
Figure 3.10	Calibration curves for TNT based on peak area using (A) the semi-logarithmic fit described in Equation 3.4 and (B) the logarithmic fit described in Equation 3.5.....	73
Figure 3.11	Calibration curves for tetryl based on peak area using (A) the semi-logarithmic fit described in Equation 3.4 and (B) the logarithmic fit described in Equation 3.5.....	74
Figure 3.12	Calibration curves for picric acid based on peak area using (A) the semi-logarithmic fit described in Equation 3.4 and (B) the logarithmic fit described in Equation 3.5.....	75
Figure 3.13	Calibration curves for RDX based on peak area using (A) the semi-logarithmic fit described in Equation 3.4 and (B) the logarithmic fit described in Equation 3.5.....	77
Figure 3.14	Calibration curves for HMX based on peak area using (A) the semi-logarithmic fit described in Equation 3.4 and (B) the logarithmic fit described in Equation 3.5.....	78
Figure 3.15	Calibration curves for NG based on peak area using (A) the semi-logarithmic fit described in Equation 3.4 and (B) the logarithmic fit described in Equation 3.5.....	80

Figure 3.16 Calibration curves for PETN based on peak area using (A) the semi-logarithmic fit described in Equation 3.4 and (B) the logarithmic fit described in Equation 3.5..... 81

## KEY TO ABBREVIATIONS

2,4-DNT	2,4-Dinitrotoluene
2,6-DNT	2,6-Dinitrotoluene
2-NT	2-Nitrotoluene
4-am-DNT	4-amino-2,6-Dinitrotoluene
CCD	Charge-coupled device
DPA	Diphenylamine
GSR	Gunshot residue
HMX	1,3,5,7-tetranitro-1,3,5,7-tetraazocyclooctane
MEK	Methylethylketone
NB	Nitrobenzene
NG	Nitroglycerin
ng	Nanogram ( $10^{-9}$ g)
PETN	Pentaerythritol tetranitrate
Picric acid	2,4,6-trinitrophenol
RDX	1,3,5-trinitro-1,3,5-triazocyclohexane
RSD	Relative standard deviation
S/N	Signal-to-noise
S/B	Signal-to-background
Tetryl	2,4,6,N-tetranitro-N-methylaniline
THF	Tetrahydrofuran
TLC	Thin-Layer Chromatography
TNT	2,4,6-Trinitrotoluene
UV	Ultraviolet
$\mu$ g	Microgram ( $10^{-6}$ g)

## CHAPTER 1. INTRODUCTION

In recent years, the determination of nitrated explosives has become increasingly important in the forensic community. In cases of national security or on the front lines of international conflicts, sophisticated technologies for explosives detection are available and widely used. For less prominent cases, however, state and local law enforcement and forensic laboratories are not equipped with state-of-the-art equipment such as handheld explosives sensors or dedicated instrumentation for explosives detection. One of the most common preliminary screening techniques used in these situations is thin-layer chromatography (TLC) with spray reagents, followed by visual inspection.<sup>1-3</sup> This project has sought to improve the TLC separation of nitrated explosives using less toxic mobile phases to decrease safety concerns while maintaining the inherent simplicity. In addition, a fluorescence quenching method has been utilized for quantitation of nitrated explosives and degradation products in a single step following TLC separation. This method offers several advantages over colorimetric methods for the detection of nitrated explosives following TLC, and can be performed with commonly-used equipment such as a handheld UV light source and a digital camera. This method provides qualitative and quantitative information simultaneously, and the sample can be preserved on the TLC plate and extracted from the stationary phase for further analysis in its original form.

## 1.1 Explosives

Nitrated explosives are divided into groups according to their use, where high explosives are described as detonating charges and low explosives as propellants.<sup>1</sup> The distinction arises because high explosives detonate at velocities in km/s, while propellants burn instead of detonating at velocities of cm/s to m/s.<sup>2,4</sup> Low explosives are used to initiate a more powerful explosive reaction by transferring energy to the main explosive charge. Because the burning rate of low explosives increases rapidly with pressure, they are also found as propellants in ammunition cartridges.<sup>2</sup> Two common low explosives are black powder (nitrate salt, charcoal, and often sulfur) and smokeless powder (nitrocellulose and possibly nitroglycerin and nitroguanidine).<sup>1,4,5</sup> High explosives or detonating charges are usually shock initiated, and are divided further to reflect their chemical composition as either organic or inorganic. Inorganic explosives are common in homemade explosive devices, as ammonia-based explosives can be easily formulated from fertilizers.<sup>2,4</sup> For example, the devices used in the 1993 World Trade Center bombing and the 1995 Oklahoma City bombing were created from ammonia-based fertilizers.<sup>6,7</sup> Ammonium nitrate is one example of a common inorganic explosive.<sup>4</sup>

Organic nitrated explosives are of greatest interest in this project because these materials are very common and comprise a majority of military and industrial explosives.<sup>2,4</sup> Organic explosives are divided into three classes based on the atom to which the nitro group (NO<sub>2</sub>) is attached. Common nomenclature and abbreviations for the explosives of interest are given in Table 1.1, and

**Table 1.1.** Explosives and degradation products used to validate TLC separation and CCD imaging system.

<b>Compound</b>	<b>Explosive Class</b>	<b>Abbreviation</b>
2,4,6-Trinitrotoluene (1)	Nitroaromatic	TNT
2,4,6-Trinitrophenol (2)	Nitroaromatic	Picric acid
2,4,6,N-Tetranitro-N-methylaniline (3)	Nitroaromatic/Nitramine	Tetryl
1,3,5-Trinitro-1,3,5-triazacyclohexane (4)	Nitramine	RDX
1,3,5,7-Tetranitro-1,3,5,7-tetraazacyclooctane (5)	Nitramine	HMX
Nitroglycerin (6)	Nitrate ester	NG
Pentaerythritol tetranitrate (7)	Nitrate ester	PETN
Nitrobenzene (8)	Degradation product	NB
2-Nitrotoluene (9)	Degradation product	2-NT
2,4-Dinitrotoluene (10)	Degradation product	2,4-DNT
2,6-Dinitrotoluene (11)	Degradation product	2,6-DNT
4-Amino-2,6-dinitrotoluene (12)	Degradation product	4-am-DNT

structures are given in Figure 1.1. Nitroaromatic explosives contain nitro groups attached to aromatic carbon atoms and include explosives such as TNT and picric acid. Nitramine explosives contain nitro groups attached to nitrogen atoms and include RDX and HMX. Tetryl is a unique explosive compound in that it has both nitroaromatic and nitramine character (Figure 1.1). Nitrate ester explosives contain nitro groups attached to oxygen atoms and include NG and PETN. In many cases, particularly when investigating aged explosive materials or those that have been detonated, degradation products will also be identified. Many degradation products are also synthetic by-products, and may be found in even recently manufactured explosive materials. Because TNT is the most commonly encountered aromatic explosive,<sup>2,4</sup> its degradation products may therefore be important in a forensic investigation. Structures of some common nitroaromatic degradation products of TNT used in this work are given in Figure 1.2.

Military explosives often consist of combinations of various organic and inorganic explosives, as shown by the examples listed in Table 1.2.<sup>1</sup> The relative percentage of individual components in each mixture varies slightly between manufacturers and also between batches from the same manufacturer. In addition to variation in composition, inert binders such as plasticizers, putties, or rubbers are added to military explosives to increase mechanical strength, stability, and lifetime of the materials.<sup>4</sup> In their crystalline forms, many explosives are not easily pressed or are highly shock sensitive. The addition of a binder to manufactured materials allows the explosive to be formed into any size or shape, as well as prevent accidental detonation through handling and transport.

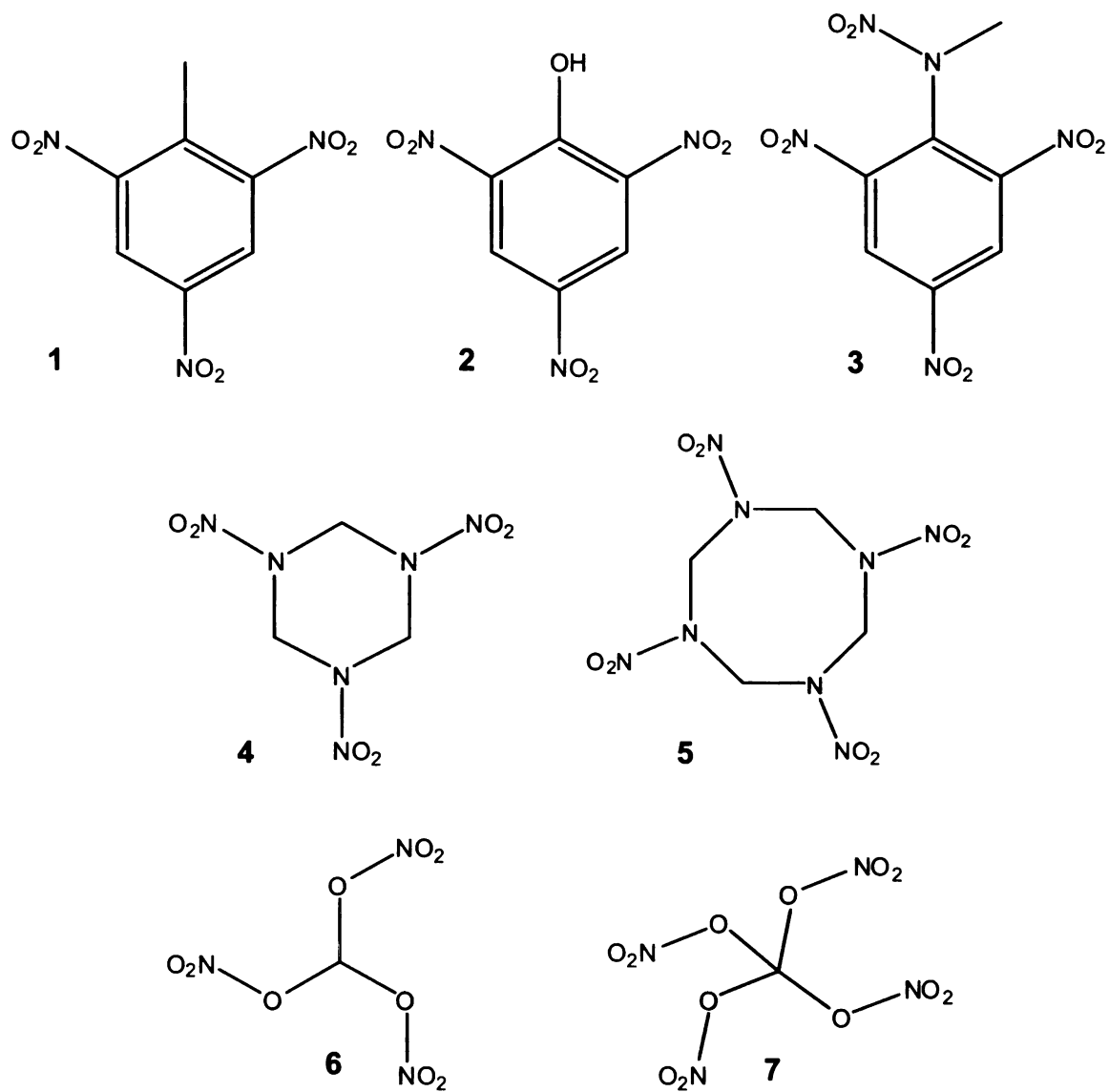


**Figure 1.1.** Common nitroaromatic explosives: (1) TNT, (2) picric acid, and (3) Tetryl. Nitramine explosives: (3) Tetryl, (4) RDX, and (5) HMX. Nitrate ester explosives: (6) NG and (7) PETN.

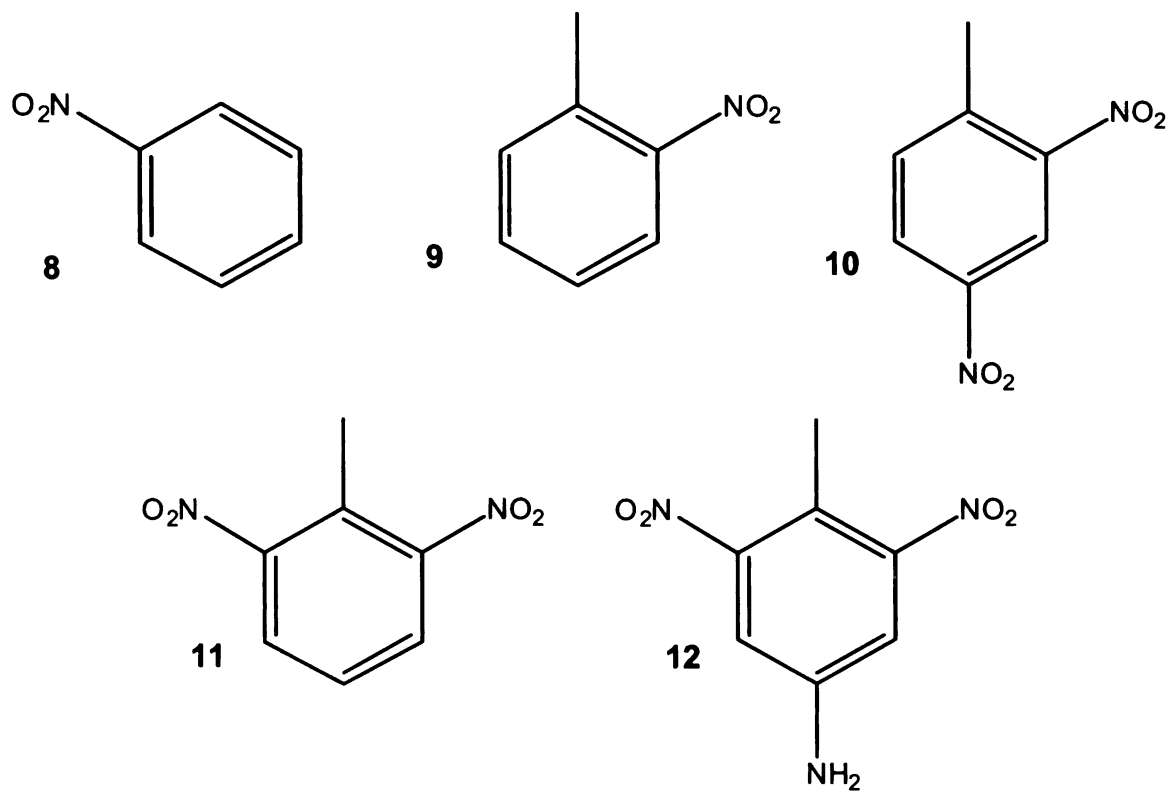


**Figure 1.2.** Some common degradation products of TNT used in this work: (8) NB, (9) 2-NT, (10) 2,4-DNT, (11) 2,6-DNT, and (12) 4-am-DNT.

**Table 1.2.** Common military explosives and formulations.<sup>1</sup>

<b>Common Name</b>	<b>Formulation</b>
Amatol	TNT + ammonium nitrate
Composition B	RDX + TNT + wax
Composition C-2	RDX + TNT +DNT + NT + nitrocellulose + dimethylformamide
Composition C-3	RDX + TNT +DNT + NT + Tetryl + nitrocellulose
Composition C-4	RDX + polyisobutylene + di(2-ethylhexyl)sebacate + fuel oil
Cyclotol	RDX + TNT
Detasheet	PETN + plasticizer
Octol	HMX + TNT
Pentolite	PETN + TNT
PTX-1	RDX + TNT + Tetryl
PTX-2	RDX + TNT + PETN
Tetrytol	TNT + Tetryl

Homemade explosive devices are often packaged in metal or glass to increase detonation power of the explosive or to increase the damage caused by added shrapnel.<sup>3</sup> All explosives, legally manufactured or illicitly assembled, may be housed in a variety of casings, for the purpose of confinement, transport, or concealment.<sup>3</sup>

## **1.2 Explosives as Evidence**

Explosives are an important class of forensic evidence, and their detection is instrumental in many criminal investigations. Undoubtedly, the most common type of explosive encountered in the forensic laboratory is smokeless powder in the form of gunshot residue (GSR). In 2003, the US Bureau of Justice Statistics reports over 366,000 victims of firearm-related crimes,<sup>8</sup> including over 10,000 homicide victims.<sup>9</sup> Comparatively, less than 400 bombings were reported by the US Bureau of Alcohol, Tobacco, Firearms, and Explosives in that same year.<sup>10</sup> Common analyses involve identification of GSR on the hands or clothing of a suspect indicating that a gun was recently fired, as well as identification of GSR on a target to identify bullet holes.<sup>2</sup>

In transportation security, passengers and baggage are screened for the presence of explosive residues prior to commercial travel. Many federal and state government buildings also require similar screening of visitors and employees. These preliminary screening methods are used to identify low levels of explosive residues present on a person or object, which may be critical to the prevention of a dangerous and life-threatening incident. In the case of a successful bombing or explosion, analysis of post-blast residues can provide

information about the type and source of the explosive used. In both cases, rapid and accurate determination of trace explosive materials is a critical step in the investigative process. In the absence of explosive material, the presence of degradation products may indicate the type or manufacturer of the explosives that was used. In many cases, degradation products have higher vapor pressures than related explosive compounds, increasing their vapor concentration and thus their ability to be detected.

### **1.3 Established Methodologies**

Forensic detection of explosives and explosives residues is multi-faceted. In the rare case that an explosive device is discovered intact, the analysis involves a simple confirmation of the identity of the explosive. As a preventative security measure, explosive residues, particles, and vapors must be identified against a complex environmental background, demanding increased selectivity. In a third scenario, explosive compounds must be identified in complex post-blast residues containing ambient air, soot, or ash. Other matrix components may include degradation products that form during production, storage, or the explosion itself. In many instances, a separation method is often used to isolate explosive materials from the complex matrix within which they are contained. Many methods have been used for such separations, including TLC,<sup>1,5</sup> gas chromatography (GC),<sup>1,5,11-15</sup> supercritical fluid chromatography (SFC),<sup>1,16</sup> liquid chromatography (LC),<sup>1,5,11,17-20</sup> ion chromatography (IC),<sup>1,21</sup> capillary electrophoresis (CE),<sup>22,23</sup> capillary electrochromatography (CEC),<sup>24</sup> and micellar electrokinetic chromatography (MEKC).<sup>25,26</sup>

In addition to separation of explosives and residues from the surrounding environment, a sensitive and selective detection method is also important. To this end, detection and characterization of nitrated explosives in the laboratory have been accomplished by colorimetric reactions,<sup>1,5,27</sup> densitometry,<sup>1,5</sup> UV absorbance,<sup>1,5,17-20,28</sup> infrared spectroscopy (IR),<sup>5,29,30</sup> nuclear magnetic resonance (NMR),<sup>1,5</sup> electrochemistry,<sup>1,5,20</sup> immunoassay,<sup>1,5,23,31-33</sup> mass spectrometry (MS),<sup>1,34-36</sup> ion mobility spectrometry (IMS),<sup>1,34-36</sup> chemiluminescence,<sup>13-15,37-40</sup> indirect laser-induced fluorescence (ILIF),<sup>24-26,41</sup> and fluorescence quenching.<sup>28,42-50</sup> Unfortunately, many of these methods are difficult to adapt for field use owing to the size of laboratory-scale instrumentation and the need for other accessories, such as large magnets for NMR or vacuum systems for MS, that limit portability.

As mentioned previously, in cases of national security or on the front lines of international conflicts, sophisticated field technologies for explosives detection are available and widely used. The most common methods for on-site explosives detection involve trained canines,<sup>51</sup> ion mobility spectrometry,<sup>34</sup> chemiluminescence,<sup>38</sup> or fluorescence quenching of amplified polymers.<sup>52</sup> Detection systems based on these methods are often costly, and for smaller, less frequent investigations, impractical. Despite the success of more sophisticated separation techniques in a laboratory setting, TLC continues to be widely used in the routine analysis of explosives because it is more rapid, portable, and inexpensive than more complex methods.

## **1.4 Thin-Layer Chromatographic Analysis of Explosives**

Thin-layer chromatography, or TLC, is a separation method that involves a thin, even layer of sorbent material deposited on a firm support, such as a glass or plastic plate.<sup>53</sup> The sorbent material, or stationary phase, consists of small silica or alumina particles and is typically deposited in a layer that is 0.10 to 0.25 mm in thickness. The compounds, or solutes, to be separated are deposited from solution near one edge of the plate. The plate is then placed into a small volume of mobile phase, which carries the solutes through the stationary phase by capillary action. Separation of the solutes is based on their affinity for the stationary phase relative to that of the mobile phase. Highly retained solutes will remain near their original location, while less retained solutes will travel with the mobile phase up the plate. The identity of a solute is determined from a comparison of the distance traveled to that of a standard material on the same plate.

Commonly, separation of explosives by TLC involves the use of toxic and/or carcinogenic mobile phases.<sup>1,5</sup> Chloroform, carbon tetrachloride, methylene chloride, and toluene are often used, either individually or in combination with other mobile phases, because they maximize resolution of the solutes in the shortest development time.<sup>5</sup> Despite their toxicity, these mobile phases have been routinely used in a variety of combinations to separate all classes of explosives.<sup>2,54-59</sup> These mobile phases pose numerous health risks and often require use of a fume hood to minimize exposure to harmful vapors.<sup>60</sup> The need for a fume hood as well as danger of accidental mobile phase spills

limits the practicality of these mobile phases for field analysis. Identification of a non-toxic alternative would be an improvement in safety and convenience in the forensic science community.

### **1.5 Detection of Explosives Following Thin-Layer Chromatography**

Detection following TLC separation is typically accomplished by using a colorimetric reaction for qualitative analysis and densitometry for quantitative analysis.<sup>1,5</sup> Colorimetric reactions are conducted on the TLC plate by spraying a reagent mixture onto the plate and often accelerating the reaction through application of a UV light. For nitrated explosives, the Griess and diphenylamine (DPA) tests are most commonly employed.<sup>1,5,61</sup> In the Griess test, nitrite ions ( $\text{NO}_2^-$ ) are first liberated from nitrate-containing explosives by reaction with base. Acidic sulfanilamide reacts with nitrites to form a diazonium salt, which in turn reacts with naphthylamine to form a pink azo dye. Visual detection limits of 5-20 ng for tetryl, RDX, HMX, NG, and PETN are reported using the Griess spray test following TLC.<sup>54</sup> In the DPA test, acidic DPA reacts with nitrites, nitrates, and other oxidizing agents to form a blue compound. Detection limits of 1  $\mu\text{g}$  are reported for inorganic nitrites following TLC using the DPA color test.<sup>1</sup> The relative lack of specificity of the DPA test, however, makes the Griess test more favorable and therefore more commonly used.

Although spot tests can indicate the presence or absence of explosives, visual inspection of the colored product on the TLC plate does not provide accurate quantitation of the compounds of interest. For explosives analysis, quantitation and knowledge of method detection limits are necessary for

evaluating utility of a technique. By measurement of the absorbance of a derivatized solute zone at a given wavelength, the concentration can be approximated by using Beer's Law.<sup>53</sup> Because the stationary phase is opaque, most densitometers operate in reflectance mode, measuring the amount of light reflected from the surface of the plate. In contrast, a typical absorbance measurement involves quantification of the amount of light transmitted through the sample. Densitometry detection limits of 0.1  $\mu\text{g}$  TNT/sample in human urine<sup>62</sup> and 2  $\mu\text{g}$  RDX/sample in manufactured explosives<sup>63</sup> have been reported. Linear dynamic ranges for densitometry have been reported as 100 – 1000  $\mu\text{g}$  TNT/sample in urine,<sup>62</sup> 1-10  $\mu\text{g}$  RDX/sample,<sup>63,64</sup> and 1-15  $\mu\text{g}$  PETN/sample in standard materials,<sup>64</sup> respectively.

Although coupling of derivatization and densitometry is sufficient in many cases, the colorimetric reagent alters the chemical composition of the nitrated explosive, prohibiting further analysis in its original form. Many colorimetric reagents require 10-60 minutes of exposure to UV light and all require a second step using densitometry for accurate quantitation. In addition, inhalation of or skin exposure to DPA or Griess reagents is known to cause organ irritation and damage.<sup>65-67</sup> Consequently, development of a non-destructive, rapid, and simple quantitation method would greatly improve the current status of nitrated explosive analysis by TLC.

An alternative method to derivatization and densitometry for detection of nitrated explosives is the use of trivial fluorescence quenching. Many TLC stationary phases contain an embedded UV-active fluorophore such as

manganese-activated zinc (~2% Zn, ~0.5% Mn). A solute that absorbs either excitation or emission light will appear as a dark spot against the fluorescent background of the plate. The dark spots are an example of trivial fluorescence quenching, arising from primary or secondary filtering of the fluorescence by a quencher molecule.<sup>68</sup> Primary filtering results from absorption of the excitation light from the source by another molecule before reaching the fluorophore. Secondary filtering results from absorption of the emitted light from the fluorophore by another molecule before reaching the detector.<sup>68</sup> In both cases, trivial quenching is related to absorptive processes and the observed decrease in fluorescence power can be related logarithmically to the concentration or mass of the quencher through a form of Beer's Law.

Although densitometers are capable of quantitating fluorescence quenching as well as absorbance or reflectance, a laboratory must purchase a densitometer and the relevant light source for such analyses. An alternative method involves imaging of the TLC plate fluorescence under a handheld UV lamp by using a digital camera. Photographic software can be used to quantitate the amount of light reaching the camera at each pixel location. Simon and coworkers demonstrated this method previously for the quantitative analysis of several organic pharmaceuticals, including acetaminophen, caffeine, and acetylsalicylic acid, following TLC.<sup>69</sup> The linear range for this method extended from the detection limit to 450 ng, with detection limits of 4.2 ng, 12.5 ng, and 71.1 ng for acetaminophen, caffeine, and acetylsalicylic acid, respectively. For on-site detection of explosives, this method is favorable because the sample is

retained in its original form and can be extracted from the stationary phase for further analyses. In addition, handheld UV lamps and digital cameras are standard equipment in all forensic laboratories, making this method easy to implement with existing technology. Furthermore, the use of this method does not preclude the use of colorimetric reagents, because the presence of the fluorophore on the TLC plate does not alter the results of the Griess or DPA tests.

## **1.6 Research Objectives**

The main objective of this research project was to identify safe, simple, and cost-effective improvements for the determination of nitrated explosives by using TLC. The first goal was to identify and characterize a less-toxic mobile phase system that would allow resolution of nitrated explosives in the fewest possible steps. The second goal was to optimize the CCD camera imaging system to ensure that the highest quality data could be extracted from TLC plate images. The final goal was to quantitate various nitrated explosives and degradation products to determine the analytical figures of merit for this detection method. Through the work presented here, the forensic science community will be able to easily adapt current technology to improve their analysis of forensic explosive evidence.

## 1.7 References

1. Yinon, J.; Zitrin, S. *Modern Methods and Applications in Analysis of Explosives*; Wiley: Chichester, West Sussex, 1993.
2. Midkiff, C. *Arson and Explosive Investigation*; Prentice-Hall: Englewood Cliffs, NJ, 1982.
3. Brodie, T. G. *Bombs and Bombings: A Handbook to Detection, Disposal, and Investigation for Police and Fire Departments*, 2nd ed.; Charles C. Thomas: Springfield, IL, 1996.
4. Cooper, P. W.; Kurowski, S. R. *Introduction to the Technology of Explosives*; VCH Publishers, Inc.: New York, NY, 1996.
5. Yinon, J.; Zitrin, S. *The Analysis of Explosives*; Pergamon: Elmsford, NY, 1981.
6. Guterl, F. *The Chemistry of Mass Murder - Homemade Fertilizer Bomb Used in Oklahoma City Bombing - 1995: The Year in Science - Brief Article*, Discover, January 1996.
7. Knight, J. In *Encyclopedia of Espionage, Intelligence, and Security*, Lerner, K. L., Lerner, B. W. Eds. World Trade Center, 1993 Terrorist Attack; Gale Group: Detroit, 2004.
8. Bureau of Justice Statistics. National Crime Victimization Survey, 2006. <http://www.ojp.usdoj.gov/bjs/glance/tables/firearmnonfataltab.htm> (accessed 10/02/07).
9. US Federal Bureau of Investigation. Supplementary Homicide Reports, 2006. <http://www.ojp.usdoj.gov/bjs/homicide/tables/weaponstab.htm> (accessed 10/02/07).
10. US Bureau of Alcohol Tobacco Firearms and Explosives. Explosive Incidents Report for Bombing - January 2003 to December 2003, 2004. <http://www.atf.gov/aaxis2/bombingrpts/bombings2003.pdf> (accessed 10/02/07).
11. Oxley, J.; Smith, J.; Resende, E.; Pearce, E. *J. Forensic Sci.* **2003**, *48*, 742-753.
12. Brown, H.; Kirkbride, K.; Pigou, P.; Walker, G. *J. Forensic Sci.* **2004**, *49*, 215-221.
13. Crowson, C. A.; Cullum, H.; Hiley, R. W.; Lowe, A. *J. Forensic Sci.* **1996**, *41*, 980-989.

14. Bowerbank, C. R.; Smith, P. A.; Fetterolf, D. D.; Lee, M. L. *J. Chromatogr. A* **2000**, *902*, 413-419.
15. Batlle, R.; Carlsson, H.; Tollback, P.; Colmsjo, A.; Crescenzi, C. *Anal. Chem.* **2003**, *75*, 3137-3144.
16. Douse, J. M. F. *J. Chromatogr. A* **1988**, *445*, 244-250.
17. Gholamian, F.; Chalooosi, M.; Husain, S. W. *Prop. Expl. Pyrotech.* **2002**, *27*, 31-33.
18. Gates, P.; Furlong, E.; Dorsey, T.; Burkhardt, M. *Trends Anal. Chem.* **1996**, *15*, 319-325.
19. Monteil-Rivera, F.; Paquet, L.; Deschamps, S.; Balakrishnan, V. K.; Beaulieu, C.; Hawari, J. *J. Chromatogr. A* **2004**, *1025*, 125-132.
20. Spiegel, K.; Welsch, T. *Fresenius J. Anal. Chem.* **1997**, *357*, 333-337.
21. Reutter, D.; Buechele, R.; Rudolph, T. *Anal. Chem.* **1983**, *55*, 1468A-1472A.
22. Casamento, S.; Kwok, B.; Roux, C.; Dawson, M.; Doble, P. *J. Forensic Sci.* **2003**, *48*, 1075-1083.
23. Bromberg, A.; Mathies, R. A. *Anal. Chem.* **2003**, *75*, 1188-1195.
24. Bailey, C. G.; Wallenborg, S. R. *Electrophoresis* **2000**, *21*, 3081-3087.
25. Wallenborg, S. R.; Bailey, C. G. *Anal. Chem.* **2000**, *72*, 1872-1878.
26. Kennedy, S.; Caddy, B.; Douse, J. M. F. *J. Chromatogr. A* **1996**, *726*, 211-222.
27. Stevanovic, S.; Mitrovic, M. *Int. J. Environ. Anal. Chem.* **1990**, *40*, 69-76.
28. Goodpaster, J. V.; McGuffin, V. L. *Anal. Chem.* **2001**, *73*, 2004-2011.
29. Pristera, F.; Halik, M.; Castelli, A.; Fredericks, W. *Anal. Chem.* **1960**, *32*, 495-508.
30. Conduit, C. P. *J. Chem. Soc.* **1959**, 3273-3277.
31. Wilson, R.; Clavering, C.; Hutchinson, A. *Anal. Chem.* **2003**, *75*, 4244-4249.
32. Narang, U.; Gauger, P. R.; Ligler, F. S. *Anal. Chem.* **1997**, *69*, 1961-1964.

33. Charles, P. T.; Rangasammy, J. G.; Anderson, G. P.; Romanoski, T. C.; Kusterbeck, A. W. *Anal. Chim. Acta* **2004**, *525*, 199-204.
34. Eiceman, G. A.; Stone, J. A. *Anal. Chem.* **2004**, *76*, 390A-397A.
35. Buryakov, I. A. *J. Chromatogr. B* **2004**, *800*, 75-82.
36. Miller, C. J.; Glenn, D. F.; Hartenstein, S. D. *Proc. SPIE-Int. Soc. Opt. Eng.* **1998**, *3575*, 335-341.
37. Jimenez, A. M.; Navas, M. J. *J. Hazard. Mater.* **2004**, *106*, 1-8.
38. Fine, D. H.; Wendel, G. J. *Proc. SPIE-Int. Soc. Opt. Eng.* **1993**, *2092*, 131-136.
39. Nguyen, D. H.; Locquiao, S.; Huynh, P.; Zhong, Q.; He, W.; Christensen, D.; Zhang, L.; Bilkhu, B. In *Electronic Noses & Sensors for the Detection of Explosives*; Gardner, J. W., Yinon, J., Eds.; Kluwer Academic Publishers: Netherlands, 2004, pp 71-80.
40. Lafleur, A. L.; Mills, K. M. *Anal. Chem.* **1981**, *53*, 1202-1205.
41. Woltman, S. J.; Even, W. R.; Sahlin, E.; Weber, S. G. *Anal. Chem.* **2000**, *72*, 4928-4933.
42. Lu, J.; Zhang, Z. *Anal. Chim. Acta* **1996**, *318*, 175-179.
43. Focsaneanu, K.-S.; Scaiano, J. C. *Photochem. Photobiol. Sci.* **2005**, *4*, 817-821.
44. Albert, K. J.; Walt, D. R. *Anal. Chem.* **2000**, *72*, 1947-1955.
45. Kose, M. E.; Harruff, B. A.; Lin, Y.; Veca, L. M.; Lu, F.; Sun, Y. P. *J. Phys. Chem. B* **2006**, *110*, 14032-14034.
46. Zhang, S.; Lu, F.; Gao, L.; Ding, L.; Fang, Y. *Langmuir* **2007**, *23*, 1584-1590.
47. Toal, S. J.; Sanchez, J. C.; Dugan, R. E.; Trogler, W. C. *J. Forensic Sci.* **2007**, *52*, 79-83.
48. Yang, J. S.; Swager, T. M. *J. Am. Chem. Soc.* **1998**, *120*, 5321-5322.
49. Rose, A.; Zhu, Z.; Madigan, C. F.; Swager, T. M.; Bulovic, V. *Nature* **2005**, *434*, 876-879.
50. Naddo, T.; Che, Y.; Zhang, W.; Balakrishnan, K.; Yang, X.; Yen, M.; Zhao, J.; Moore, J. S.; Zang, L. *J. Am. Chem. Soc.* **2007**, *129*, 6978-6979.

51. Furton, K. G.; Myers, L. J. *Talanta* **2001**, *54*, 487-500.
52. Wang, L. *Chem. Eng. News* **2007**, *85*, 11.
53. Wall, P. E. *Thin-Layer Chromatography: A Modern Practical Approach*; The Royal Society of Chemistry: Cambridge, UK, 2005.
54. Douse, J. M. F. *J. Chromatogr. A* **1982**, *234*, 415-425.
55. Kohlbeck, J. A.; Chandler, C. D.; Bolleter, W. T. *J. Chromatogr. A* **1970**, *46*, 173-179.
56. Chandler, C. D.; Kohlbeck, J. A.; Bolleter, W. T. *J. Chromatogr. A* **1972**, *67*, 255-259.
57. Hoffsommer, J. C.; McCullough, J. F. *J. Chromatogr. A* **1968**, *38*, 508-514.
58. Hoffsommer, J. C.; Glover, D. J. *J. Chromatogr. A* **1971**, *62*, 417-421.
59. Parihar, D.; Sharma, S.; Verma, K. *J. Forensic Sci.* **1968**, *13*, 246-252.
60. Klaassen, C., 6th ed.; McGraw-Hill: New York, NY, 2001.
61. Jenkins, T.; Walsh, M. *Talanta* **1992**, *39*, 419-428.
62. Liu, Y.; Wei, W.; Wang, M.; Pu, Y.; Lin, L.; Zhang, J. *J. Planar Chromatogr.* **1991**, *4*, 146-149.
63. Gholamian, F.; Chaloosi, M.; Waquif-Husain, S.; Dehghani, H. *J. Planar Chromatogr.* **2001**, *14*, 296-299.
64. Bladek, J.; Miszczak, M.; Popiel, S. *Chem. Anal. (Warsaw)* **1995**, *40*, 723-729.
65. Diphenylamine, MSDS No D7728. Mallinckrodt Baker: Phillipsburg, NJ, February 26, 2007. <http://www.itbaker.com/msds/englishhtml/d7728.htm> (accessed 9/12/07)
66. Sulfanilamide, MSDS No S7658. Mallinckrodt Baker: Phillipsburg, NJ, May 25, 2007. <http://www.itbaker.com/msds/englishhtml/s7658.htm> (accessed 9/12/07)
67. 1,8-Diaminonaphthalene, MSDS No SLD2968. Sciencelab.com: Houston, TX, December 10, 2005. [http://www.sciencelab.com/xMSDS-1\\_8\\_Diaminonaphthalene-9927150](http://www.sciencelab.com/xMSDS-1_8_Diaminonaphthalene-9927150) (accessed 9/12/07)
68. McGuffin, V. L.; Goodpaster, J. V. In *Encyclopedia of environmental analysis and remediation.*; Meyers, R., Ed.; Wiley: New York, NY, 1998, pp 3815-3831.

69. Simon, R. E.; Walton, L. K.; Liang, Y.; Denton, M. B. *Analyst* **2001**, *126*, 446-450.

## **CHAPTER 2. SEPARATION OF NITRATED EXPLOSIVES**

The TLC separation of nitrated explosives and degradation products was accomplished using mobile phase systems that are less toxic than those currently in use. An analysis procedure was developed to separate an unknown explosive sample containing up to 12 explosives in two steps. In the first analysis step, nitroaromatic and nitrate ester explosives can be separated and identified, while picric acid and nitramine explosives are analyzed in the second step. This method was successfully applied in the analysis of two blind samples.

### **2.1 Experimental Methods**

#### **2.1.1 Chemicals**

Conventional manganese-activated zinc silicate TLC plates (Silica gel 60, 5x10 cm and 5x20 cm, 150-Å pores, 250-µm layer thickness, Whatman, Florham Park, NJ) were used for explosives separation. Reagent and spectral grade solvents used in TLC plate preparation and explosives separation included acetone (Sigma-Aldrich, St. Louis, MO), acetonitrile (Sigma-Aldrich), benzaldehyde (Fisher Scientific, Waltham, MA), benzonitrile (Eastman Organic, Rochester, NY), cyclohexane (Sigma-Aldrich), hexane (Honeywell Burdick & Jackson, Morristown, NJ), methanol (Sigma-Aldrich), methylene chloride (Spectrum, Gardena, CA), methylethylketone (Columbus Chemical Industries, Columbus, WI), pentane (Jade Scientific, Canton, MI), tetrahydrofuran (Spectrum), and triethylamine (Spectrum). Analytical standards of 2-NT, 4-NT, 2,4-DNT, 2,6-DNT, 4-am-DNT, TNT, tetryl, picric acid, HMX (Sigma-Aldrich),

RDX, NG, PETN (Radian, Austin, TX), and NB (Mallinckrodt, Hazelwood, MO) were used as received in methanol or acetonitrile solution. Standard solutions ( $10^{-1}$  to  $10^{-4}$  M) were prepared for each explosive in spectroscopic grade methanol or acetonitrile (Honeywell Burdick & Jackson). Working concentrations and application volume of the nitrated explosives solutions were chosen for TLC analysis to yield solute zones visible to the eye under UV irradiation.

### **2.1.2 Plate Preparation**

Prior to chromatographic analysis, plates were pretreated to remove loose particles and contamination that may lead to irreproducible retention or fluorescence backgrounds. The TLC development chamber (Kodak, Rochester, NY) used for plate pretreatment consisted of a glass mobile phase reservoir and two textured glass plates between which the TLC plates were placed during the washing step. Plates were incubated in pure solvent in the development chamber for 1 hour and heated at 90 °C for at least 24 hours to remove residual solvent or adsorbed compounds. Plates were stored in the 90 °C oven until use to prevent adsorption of water or other contaminants from the laboratory environment that may deactivate the silica.

Several common solvents of varying solvent strength were investigated for use in plate pretreatment, including acetone, acetonitrile, hexane, methanol, and methylene chloride. Test plates were partially developed in each solvent and the fluorescence was observed for the washed and unwashed sections of each plate. Upon visual comparison, plates developed in acetonitrile, hexane, and methanol had equivalent fluorescence after washing, while the fluorescence of plates

cleaned using acetone and methylene chloride had significantly less fluorescence. In addition, a build-up of contamination at the solvent front was observed on plates cleaned in acetonitrile and methanol that was not observed on plates washed in hexane. The visible build-up indicated greater removal of non-fluorescent compounds from plates washed in methanol and acetonitrile. In consideration of application to field use by forensic scientists, methanol is a better choice of solvent because the cost of acetonitrile is approximately 2.5 times greater than that of methanol. For these reasons, methanol was used for plate pretreatment for all subsequent measurements.

Standard solutions were applied in 5  $\mu\text{L}$  increments  $\sim 1$  cm from the bottom of cleaned plates using a capillary tube (PCR Micropipettes, to deliver 1-5  $\mu\text{L}$ , Drummond, Broomall, PA). Application was repeated in 5- $\mu\text{L}$  increments until the desired mass of solute was reached. An alternative method in which solutes were applied using a 10- $\mu\text{L}$  syringe (Hamilton, Reno, NV) was found to be more time intensive than using a capillary tube. The increase in time required for application with the syringe allowed evaporation of volatile solutes (e.g., nitrobenzene) and resulted in decreased signal for the same solute concentration compared to the capillary tube application.

### **2.1.3 Plate Development**

An enclosed developing chamber (Desaga, Heidelberg, Germany) was used for development of plates after solute application. The glass lid was sealed to prevent loss of mobile phase vapors and to allow plate development under equilibrium conditions. Plates were placed inside the apparatus such that the

mobile phase level was less than 1 cm from the bottom of the plate. Plates were developed until the mobile phase front reached 1 cm from the top (Figure 2.1, a and b). The plate was removed from the development chamber and the mobile phase was allowed to evaporate. A handheld UV lamp (254 nm, Ultraviolet Products, Upland, CA) was then used to visualize the solutes on the plate, seen as dark zones against a fluorescent background (Figure 2.1, c-f). The distance traveled by the solute was measured from the center of the zone at both the initial and final locations on the plate. Relative solute retention was determined by comparison of calculated retention factors, or  $R_f$  values, as described by Equation 2.1.

$$R_f = \frac{\text{solute distance}}{\text{solvent front distance}} \quad (2.1)$$

Solutes that are highly retained and remain near the original location will have small  $R_f$  values, near zero. Solutes that are non-retained or travel to the solvent front will have large  $R_f$  values, near unity.

## 2.2 Theory of Adsorption Chromatography

The retention of any compound in TLC depends primarily on the relative adsorption energies of the functional groups within the solutes. The  $Q_i^0$  parameter is a dimensionless representation of the free energy of adsorption for a functional group  $i$ .<sup>1</sup> Values of  $Q_i^0$  depend on the nature of the functional group and are different for substituents on aliphatic, aromatic, and combined aliphatic and aromatic backbones (Table 2.1). Assuming that each substituent is independent, the energy of adsorption for each nitrated explosive is estimated by

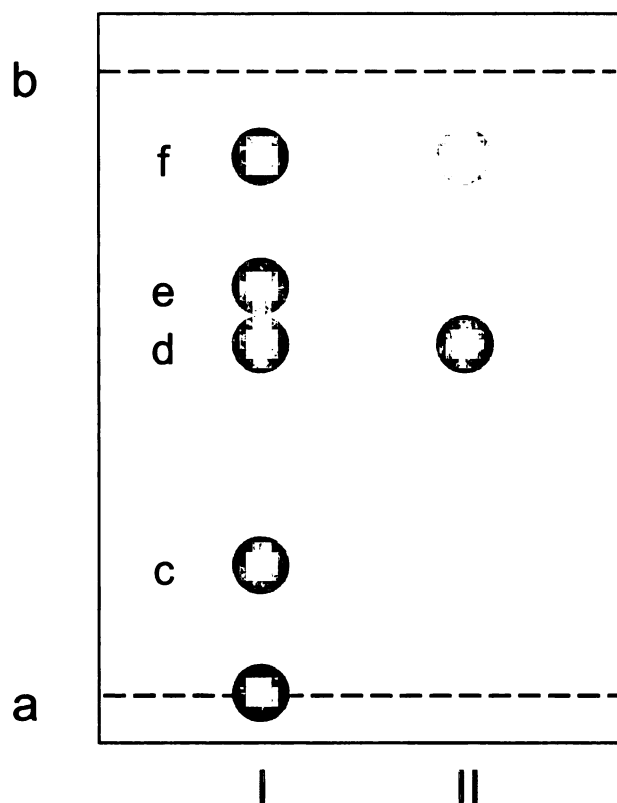


**Figure 2.1.** Sample plate containing (I) a reference sample and (II) an unknown sample. Designated plate areas include (a) the original location and a completely retained solute ( $R_f = 0$ ), (b) the solvent front, (c,e) a solute ( $R_f(c) = 0.21$ ,  $R_f(e) = 0.66$ ) that is detected in the reference sample but undetected in the unknown sample, (d) a solute ( $R_f = 0.56$ ) that is detected in both the reference and unknown samples at similar concentrations, and (f) a solute ( $R_f = 0.87$ ) that is detected at a higher concentration in the reference sample than in the unknown sample.

**Table 2.1.** Group adsorption energies for substituents common to nitrated explosives and degradation products.<sup>1</sup>

Substituent, i	Q <sub>i</sub> <sup>0</sup>	
	Aliphatic	Aromatic
Carbon (-C-)	0.25	0.25
Methylene (-CH <sub>2</sub> -)	-0.05	0.07
Methyl (-CH <sub>3</sub> )	0.07	0.11
Ether (-O-)	3.61	0.87
Hydroxyl (-OH)	5.60	4.20
Tertiary amine (-N<)	5.80	2.52 <sup>a</sup>
Primary amine (-NH <sub>2</sub> )	8.00	5.10
Nitro (-NO <sub>2</sub> )	5.71	2.77

<sup>a</sup> Tertiary amine value is for mixed aliphatic-aromatic substituent.

the sum of the group adsorption energies,  $Q_i^0$  (Table 2.2).<sup>1,2</sup> When comparing two solutes, the molecule with the greater net adsorption energy will be predicted to be adsorbed most strongly and therefore most retained.

Of the substituents common to nitrated explosives, carbon-based groups contribute the least to the adsorption, while amine, hydroxyl, and nitro groups contribute most. For carbon-based functional groups, aromatic substituents have higher adsorption energies than aliphatic groups. Conversely, for stronger adsorbing groups such as those containing nitrogen or oxygen, aliphatic forms are more strongly adsorbed than aromatic groups. In addition, increasing the number of functional groups increases the adsorption of the molecule. From 2-NT to 2,6-DNT to TNT, for example, the adsorption energy increases with addition of aromatic nitro substituents ( $Q_i^0 = 2.77$ ). For 4-am-DNT, the addition of an aromatic amine substituent ( $Q_i^0 = 5.10$ ) results in increased adsorption energies relative to 2,6-DNT. Similarly for picric acid, the addition of an aromatic hydroxyl substituent ( $Q_i^0 = 4.20$ ) results in increased adsorption energies relative to TNT. Tetryl contains an additional aliphatic nitro substituent ( $Q_i^0 = 5.71$ ) and an aliphatic/aromatic tertiary amino substituent ( $Q_i^0 = 2.52$ ), also increasing the adsorption energy relative to TNT. In addition, nitramine and nitrate ester explosives are expected to be more strongly adsorbed than nitroaromatic explosives, as the group adsorption energy for aliphatic nitro substituents ( $Q_i^0 = 5.71$ ) is twice that for the same group on an aromatic molecule ( $Q_i^0 = 2.77$ ). The adsorption energies of HMX and PETN are greater than those for RDX and NG, respectively, as expected from the addition of the fourth nitro substituent.

**Table 2.2.** Net adsorption energies for explosives and degradation products.<sup>1</sup>

<b>Compound</b>	<b><math>(Q_i^0)_{net}^a</math></b>
TNT	9.92
Picric acid	14.01
Tetryl	17.99
RDX	34.38
HMX	45.84
NG	28.21
PETN	37.53
NB	4.27
2-NT	4.38
2,4-DNT	7.15
2,6-DNT	7.15
4-am-DNT	12.25

<sup>a</sup> Net values calculated according to Reference 2.

In addition to primary adsorption effects represented by  $Q_i^0$  values, secondary effects must also be considered.<sup>3</sup> Although adsorption energies calculated in this way can provide some information about relative adsorption strength, secondary structural and electronic effects are also important in molecules with substituent groups that are not independent. For example, concerted adsorption may be possible for molecules in which two non-interacting functional groups in close proximity can simultaneously interact with the surface. Concerted adsorption can enhance adsorption relative to the same groups when separated.<sup>3</sup> Conversely, interaction between groups in close proximity can reduce or prevent adsorption of either group, resulting in an antagonistic effect on adsorption relative to the same groups when separated. Electron-donating and -withdrawing substituents can also enhance or diminish adsorption by causing intramolecular inductive effects in aromatic systems. In addition, adsorption can be diminished sterically by bulky, non-interacting groups that can limit access of other substituents to surface sites. Similarly, increased linearity and planarity of molecules can lead to increased adsorption through simultaneous interaction of multiple sites with the surface. Understanding the impact of secondary effects can allow predictions about the adsorption of a group of solutes, such as nitrated explosives.

The interaction between the mobile phase and the surface must also be considered when predicting retention behavior. In adsorption chromatography, the mobile phase acts as a displacing agent during the separation. The retention therefore depends on the solvent strength parameter,  $\epsilon^0$ , of the mobile phase.

The solvent strength parameter describes the relative adsorption of a pure mobile phase on a given adsorbent. Solvent strengths are measured relative to pentane, the simplest hydrocarbon mobile phase (defined as  $\varepsilon^0 = 0$ ), where a large  $\varepsilon^0$  value implies increased displacing power.<sup>1</sup> Measured strengths for mobile phases used in this study are given in Table 2.3. When a single mobile phase cannot provide adequate separation of solutes of interest, two or more solvents can be combined to produce a mobile phase of intermediate strength. For a binary mixture of a bulk mobile phase component (a) and modifier (b), the combined solvent strength can be estimated by using Equation 2.2.<sup>1</sup>

$$\varepsilon_{ab}^0 = \varepsilon_a^0 + \frac{\log\left(X_b 10^{\alpha n_b (\varepsilon_b^0 - \varepsilon_a^0)} + 1 - X_b\right)}{\alpha n_b} \quad (2.2)$$

From Equation 2.2, the combined solvent strength parameter ( $\varepsilon_{ab}^0$ ) is related to the solvent strength parameters of the bulk mobile phase constituent ( $\varepsilon_a^0$ ) and modifier ( $\varepsilon_b^0$ ), the adsorbent activity function ( $\alpha$ , taken to be unity), the mole fraction of the modifier ( $X_b$ ), and the molecular area of the modifier ( $n_b$ ).<sup>1</sup>

### 2.3 Separation of TNT and Degradation Products

In the literature, common mobile phase mixtures used to separate nitroaromatic explosives have ranged from 7:3 cyclohexane:chloroform ( $\varepsilon_{ab}^0 = 0.17$ ) to 3:1 hexane:acetone ( $\varepsilon_{ab}^0 = 0.33$ ).<sup>4</sup> The numerical average of the  $\varepsilon^0$  values for eleven mobile phases used to separate these compounds is 0.24.<sup>4</sup> In our studies, this solvent strength was first approximated by using a mixture of 80:20 cyclohexane: MEK ( $\varepsilon_{ab}^0 = 0.25$ ). This mixture, however, did not move the

**Table 2.3.** Properties of common TLC mobile phases.<sup>5</sup>

<b>Mobile phase</b>	<b>Solvent Strength Parameter, <math>\epsilon^0</math> (SiO<sub>2</sub>)</b>	<b>Molecular Area, n (Å)</b>
Pentane	0.00	5.9
Hexane	0.03	6.0
Cyclohexane	0.03	6.0
Carbon tetrachloride	0.11	5.0
Benzene	0.25	6.0
Chloroform	0.26	5.0
Methylene chloride	0.32	4.1
THF	0.35 <sup>a</sup>	5.0
MEK	0.39 <sup>a</sup>	4.9
Acetone	0.47	4.2
Acetonitrile	0.50	10.0
Methanol	0.73	8.0

<sup>a</sup> Values estimated based on Reference 2.

solutes from their original location. A combination of 85:15 hexane:THF ( $\epsilon_{ab}^0 = 0.20$ ) is also of appropriate strength to provide sufficient separation of nitroaromatic explosives and degradation products. However, this combination did not provide sufficient resolution of TNT from NB (Figure 2.2). To determine the mobile phase composition necessary to fully resolve TNT from all degradation products, the percent THF in the mobile phase was decreased systematically from 15% to 8%, and the resulting retention factors are compared in Figure 2.2. Because THF is a stronger displacing agent than hexane, decreasing the fraction of THF decreased the  $R_f$  values for NB, 2-NT, 2,4-DNT, 2,6-DNT, and 4-am-DNT at a similar rate. The  $R_f$  value for TNT, however, decreased more dramatically in this range, overlapping NB at high percentages of THF and nearing 2,6-DNT at low percentages of THF. The optimum mobile phase for separation of nitroaromatic explosives and degradation products was 88:12 hexane:THF ( $\epsilon_{ab}^0 = 0.18$ ), which allowed separation of TNT and NB while maximizing the  $R_f$  value for 4-am-DNT, which was highly retained. Using this mobile phase composition, the observed retention order was 4-am-DNT, 2,4-DNT, 2,6-DNT, TNT, NB, and 2-NT, and the precision of  $R_f$  values are summarized in Table 2.4.

Of TNT and the degradation products, 4-am-DNT was the most retained, as expected from the calculated adsorption energies (Table 2.2). Both 2,4-DNT and 2,6-DNT were more retained than TNT, although the group adsorption energy of TNT is greater. The presence of the electron withdrawing *p*-nitro substituent of TNT (Figure 1.2) may have an intramolecular inductive effect on

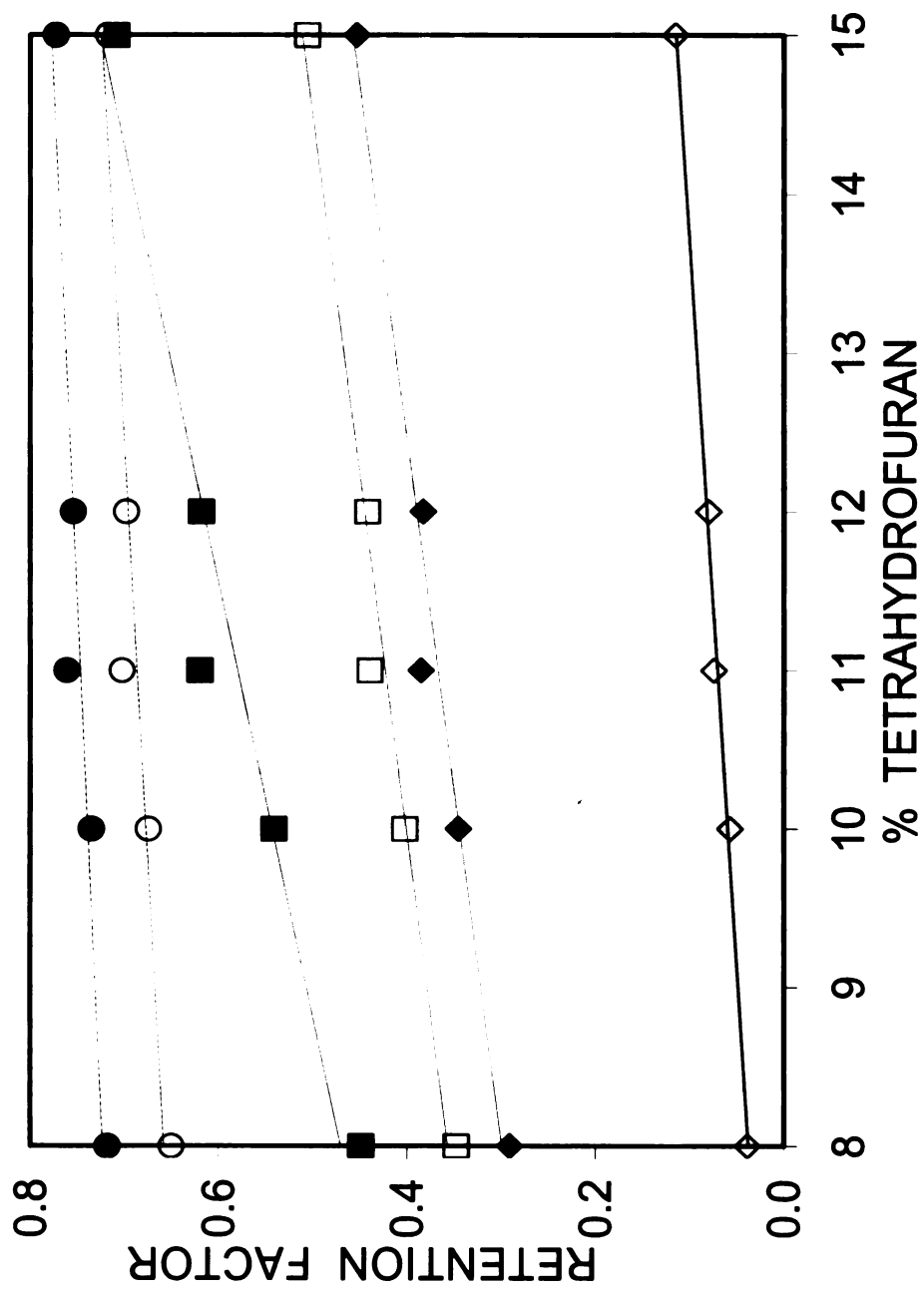


**Figure 2.2.** Effect of percent THF in hexane on the retention factors measured for TNT (■) and degradation products, including NB (○), 2-NT (●), 2,4-DNT (◆), 2,6-DNT (□), and 4-am-DNT (◇).

**Table 2.4.** The precision of retention factors for nitroaromatic explosives and degradation products in 88:12 hexane:THF.

<b>Solute</b>	<b>Retention Factor, <math>R_f</math></b>
NB	$0.698 \pm 0.007^a$
2-NT	$0.754 \pm 0.007$
2,4-DNT	$0.383 \pm 0.006$
2,6-DNT	$0.442 \pm 0.006$
4-am-DNT	$0.080 \pm 0.005$
TNT	$0.618 \pm 0.005$

<sup>a</sup> Precision calculated as the standard deviation of 8 replicate measurements.

both *o*-nitro substituents, decreasing adsorption of these groups relative to the same substituents in 2,6-DNT. In addition, simultaneous adsorption of the two *o*-nitro substituents may be sterically hindered by the presence of the methyl group, decreasing adsorption for TNT and 2,6-DNT relative to 2,4-DNT. Taken together, these secondary adsorption effects result in TNT being less retained than was predicted by the adsorption energy. This trend was also reported by Zou and coworkers in the separation of TNT, DNT, and am-DNTs in normal phase liquid chromatography using a silica stationary phase.<sup>6</sup> Lastly, although NB is predicted to be the least retained compound, 2-NT is less retained than NB. For 2-NT, the steric effect of the methyl substituent may decrease the adsorption energy of the nitro group, resulting in less than predicted retention.

## 2.4 Separation of Nitroaromatic Explosives

The effect of mobile phase composition was also investigated for the nitroaromatic explosives. Tetryl has an adsorption energy more similar to that of the nitroaromatic than nitramine explosives, and was therefore separated with the nitroaromatic compounds. A mixture of 88:12 hexane:THF ( $\epsilon_{ab}^0 = 0.18$ ) resulted in strong retention of picric acid ( $R_f = 0$ ). Picric acid was also completely retained in a mixture of 80:20 hexane:THF ( $\epsilon_{ab}^0 = 0.22$ ), while TNT traveled in the solvent front ( $R_f = 1$ ). Based on these two separations, no mixture of hexane and THF would retain TNT and cause migration of picric acid simultaneously. A combination of 70:30 cyclohexane:MEK ( $\epsilon_{ab}^0 = 0.28$ ), however, yielded less extreme retention of both picric acid and TNT. Using this mobile phase composition, the observed retention order was picric acid, tetryl, and TNT, and

the reproducibility of the retention factors is summarized in Table 2.5.

Although picric acid was most retained, tetryl was predicted to be the most retained compound based on calculated adsorption energies (Table 2.2). One explanation is that intramolecular inductive effects are possible for picric acid in which the presence of the electron-donating hydroxyl group may increase adsorption of nitro substituents. In addition, concerted adsorption of the hydroxyl and both *o*-nitro substituents may also be possible for picric acid, resulting in increased retention. Combined, these two effects may have resulted in the retention of picric acid being stronger than predicted by net adsorption energies.

## 2.5 Separation of Nitroaromatic and Nitrate Ester Explosives

In the literature, several mobile phase combinations have been used for the separation of nitrate ester explosives, ranging from 4:1 petroleum ether:dichloroethane ( $\epsilon_{ab}^0 = 0.17$ ) to 4:1 carbon tetrachloride:acetone ( $\epsilon_{ab}^0 = 0.32$ ).<sup>4</sup> The numerical average of the  $\epsilon^0$  values for seven mobile phases used to separate these compounds is 0.24.<sup>4</sup> Because this  $\epsilon^0$  value is similar to that used to separate TNT and its degradation products, a similar mobile phase of 88:12 hexane:THF ( $\epsilon_{ab}^0 = 0.18$ ) was used to separate the nitrate ester explosives from TNT. In addition, because TNT and tetryl have similar adsorption energies, separation of tetryl from TNT, NG, and PETN was also possible using this mobile phase. The observed retention order was tetryl, NG, TNT, and PETN, and the  $R_f$  values measured for these solutes are summarized in Table 2.6.

Despite the observed retention order, calculated values of adsorption energy indicate that the nitrate ester explosives should be most highly retained,

**Table 2.5.** The precision of retention factors for nitroaromatic explosives in 70:30 cyclohexane:MEK.

<b>Solute</b>	<b>Retention Factor, <math>R_f</math></b>
TNT	$0.53 \pm 0.01^a$
Tetryl	$0.40 \pm 0.02$
Picric Acid	$0.07 \pm 0.01$

<sup>a</sup> Precision is calculated as the standard deviation of 8 replicate measurements.

**Table 2.6.** The precision of retention factors for nitroaromatic and nitrate ester explosives in 88:12 hexane:THF.

<b>Solute</b>	<b>Retention Factor, <math>R_f</math></b>
TNT	$0.59 \pm 0.02^a$
Tetryl	$0.096 \pm 0.005$
NG	$0.28 \pm 0.04$
PETN	$0.78 \pm 0.02$

<sup>a</sup> Precision is calculated as the standard deviation of 8 replicate measurements.

followed by tetryl and TNT. As mentioned previously, the calculated adsorption energies assume that substituents are independent because they are bonded to aliphatic or aromatic carbon atoms, which is not the case for NG and PETN. Thus, the adsorption energies for  $-O-NO_2$  groups may be greater than those for aromatic nitro groups alone. Interestingly, PETN is less retained than NG, although PETN contains an additional  $-O-NO_2$  functionality that increases its calculated adsorption energy and predicted retention. From the construction of molecular models, it appears that concerted adsorption is more sterically favorable for NG than for PETN, therefore increasing the retention.

## 2.6 Separation of Nitramine Explosives

Compared to those used for separation of nitroaromatic and nitrate ester explosives, stronger mobile phase combinations have been reported in the literature for separation of nitramine explosives.<sup>4</sup> These mobile phase mixtures range from 10:1 chloroform:nitromethane ( $\epsilon_{ab}^0 = 0.31$ ) to 9:1 dichloromethane:acetonitrile ( $\epsilon_{ab}^0 = 0.41$ ).<sup>4</sup> The numerical average of  $\epsilon^0$  values for six mobile phases used to separate these compounds is 0.37.<sup>4</sup> Because RDX and HMX have been separated in stronger mobile phases than most nitroaromatic and nitrate ester explosives, a combination of 88:12 hexane:THF ( $\epsilon_{ab}^0 = 0.18$ ) was not sufficient for their separation, resulting in  $R_f$  values of zero for both solutes. Increasing the proportion to 75:25 hexane:THF ( $\epsilon_{ab}^0 = 0.23$ ) still resulted in unsatisfactory separation, with both solutes having similar retention factors. Increasing the proportion further to 50:50 hexane:THF ( $\epsilon_{ab}^0 = 0.29$ ) improved the separation, and the reproducibility of retention factors obtained with

this mobile phase is shown in Table 2.7. As predicted by adsorption energies, HMX was more retained than RDX.

Because picric acid was highly retained in 88:12 hexane:THF, analysis of picric acid with the nitramine explosives may be more effective in method development than analysis with nitroaromatic explosives. Using 50:50 hexane:THF ( $\epsilon_{ab}^0 = 0.29$ ), picric acid and HMX were not resolved. To increase solvent strength, a combination of 65:35 hexane:MEK ( $\epsilon_{ab}^0 = 0.30$ ) was used with a retention order of picric acid, HMX, and RDX. Measured  $R_f$  values for these solutes are summarized in Table 2.8. As predicted by the calculated adsorption energies (Table 2.2), RDX was less retained than HMX. Picric acid, however, was significantly more retained relative to RDX and HMX than predicted by calculated adsorption energies. As discussed previously, concerted adsorption of the hydroxyl and both *o*-nitro substituents may be possible for picric acid, resulting in greater than predicted retention.

## 2.7 Precision of Retention Factors

Reported in Tables 2.3-2.7 is the precision associated with replicate measurements of  $R_f$  values for each solute. For all solutes except NG, the relative standard deviation (RSD) in the  $R_f$  value was less than 8%. For weakly retained solutes ( $R_f > 0.38$ ), the RSD was less than 4%, with an average of 1.6%. For more strongly retained solutes ( $R_f < 0.38$ ), the RSD was significantly greater at 7.9%. The greatest error in measurement of  $R_f$  values in TLC resulted from accurately determining the center of the solute zone, which was increasingly difficult for weakly retained solutes. Although the magnitude of the deviation is

**Table 2.7.** The precision of retention factors for nitramine explosives in 50:50 hexane:THF.

<b>Solute</b>	<b>Retention Factor, <math>R_f</math></b>
RDX	$0.21 \pm 0.02^a$
HMX	$0.138 \pm 0.009$

<sup>a</sup> Precision is calculated as the standard deviation of 8 replicate measurements.

**Table 2.8.** The precision of retention factors for nitramine explosives and picric acid in 65:35 hexane:MEK.

<b>Solute</b>	<b>Retention Factor, <math>R_f</math></b>
Picric Acid	$0.13 \pm 0.01^a$
RDX	$0.509 \pm 0.007$
HMX	$0.32 \pm 0.02$

<sup>a</sup> Precision is calculated as the standard deviation of 8 replicate measurements.

consistent for all solutes, the RSD was greater for weakly retained solutes. The large RSD observed for NG (15%) was likely a result of both low signal and nonlinearity of the adsorption isotherm, as a high concentration was needed to accurately determine the  $R_f$  value. This combination made determination of the center of the solute zone difficult, leading to more variability in the  $R_f$  value.

## **2.8 Separation of an Unknown Explosive Sample**

Based on the mobile phase optimization studies discussed above, an analysis scheme was developed and applied for the separation of two unknown explosive mixtures. Each blind sample was applied by a volunteer onto three 5x10 cm TLC plates. The use of multiple small plates allowed rapid development and therefore reduced analysis time. Three of the nine explosive standards were also applied to the plate for direct comparison. The three plates were developed simultaneously in 88:12 hexane:THF for determination of nitrate ester and nitroaromatic explosives and degradation products in less than 10 min. By comparison of the  $R_f$  values for the unknowns with each of the standards (Table 2.9), unknown 1 was determined to contain TNT and 4-am-DNT. Unknown 2 was determined to contain 2,6-DNT (Table 2.10), as well as highly retained compounds (picric acid, HMX, or RDX) that must be separated in the second step using 65:35 hexane:MEK for the separation of nitramine explosives and picric acid. Standards of picric acid, HMX, and RDX, as well as unknown 2, were applied to a fourth plate and developed in 65:35 hexane:MEK in less than 10 min. By comparison of the  $R_f$  values for the unknown and standard samples (Table 2.10), unknown 2 was determined to contain picric acid and RDX, in addition

**Table 2.9.** Analysis of unknown explosive sample 1.

<b>Solute</b>	<b>R<sub>f</sub> Value</b>	
	<b>Standard</b>	<b>Unknown</b>
2-NT	0.74	
NB	0.68	
TNT	0.60	0.60
2,6-DNT	0.47	
2,4-DNT	0.44	
Tetryl	0.13	
4-am-DNT	0.11	0.11

**Table 2.10.** Analysis of unknown explosive sample 2.

<b>Solute</b>	<b>R<sub>f</sub> Value</b>	
	<b>Standard</b>	<b>Unknown</b>
2-NT	0.71	
NB	0.75	
TNT	0.59	
2,6-DNT	0.44	0.45
2,4-DNT	0.48	
Tetryl	0.10	
4-am-DNT	0.095	
RDX	0.62	0.61
HMX	0.44	
Picric acid	0.25	0.25

to 2,6-DNT determined in the first step. Using this method, all explosives contained in two blind samples were correctly identified with a maximum total analysis time of 30 min.

## **2.9 Conclusions**

Using the two mobile phase systems described and identified here, a two-step separation can be used to determine all of the explosives considered in this study. After application of an unknown mixture, plate development in 88:12 hexane:THF will separate nitroaromatic and nitrate ester explosives. Nitramine explosives and picric acid will remain at the original location, as the hexane:THF mobile phase is not strong enough to cause their migration. After identification and quantitation of the nitroaromatic and nitrate ester explosives, development in 65:35 hexane:MEK will provide separation of the nitramine explosives and picric acid. Using this method, up to 12 explosives and degradation products can be separated in two steps.

## 2.10 References

1. Snyder, L. *Principles of Adsorption Chromatography*; Marcel Dekker: New York, NY, 1968.
2. Barton, A. *CRC Handbook of Solubility Parameters and Other Cohesion Parameters*; CRC Press: Boca Raton, FL, 1991.
3. Lakowicz, J. *Principles of Fluorescence Spectroscopy*; Plenum Press: New York, NY, 1983.
4. Yinon, J.; Zitrin, S. *The Analysis of Explosives*; Pergamon: Elmsford, NY, 1981.
5. Snyder, L. *J. Chromatogr.* **1966**, *25*, 274-293.
6. Zou, H.; Zhou, S.; Hong, M.; Zhang, Y.; Lu, P. *Anal. Chim. Acta* **1994**, *291*, 205-210.

## CHAPTER 3. QUANTITATION OF NITRATED EXPLOSIVES

Quantitation of nitrated explosives and degradation products following TLC was accomplished by using images acquired with a computer-controlled charge-coupled device (CCD) camera. The positions of system components were adjusted for imaging of fluorescent TLC plates under UV irradiation, where areas containing solute zones were dark against a fluorescent background. The settings associated with image acquisition and manipulation were also investigated to ensure collection of the highest quality data. Using the software associated with the camera, images were corrected for illumination gradients. The peak height and area of each dark zone were correlated to the mass of solute using both a semi-logarithmic and logarithmic relationship. Explosives were quantitated over three orders of magnitude with practical detection limits in the low microgram ( $\mu\text{g}$ ) range. This method was successfully applied for the quantitation of two blind samples.

### 3.1 Positioning of Imaging System Components

An uncooled, computer-controlled CCD camera (model DXM1200F, Nikon, Melville, NY) was used to image TLC plates under continuous illumination by two mercury lamps (254 nm, Ultraviolet Products, Upland, CA) (Figure 3.1). Illumination by UV lamps resulted in a fluorescent green background of the plate with darkened zones that correspond to the solute locations. The relative positions of the system components were adjusted to maximize fluorescence from the plate as well as provide consistency between consecutive measurements. The fluorescence power of the TLC plate was dependent on the

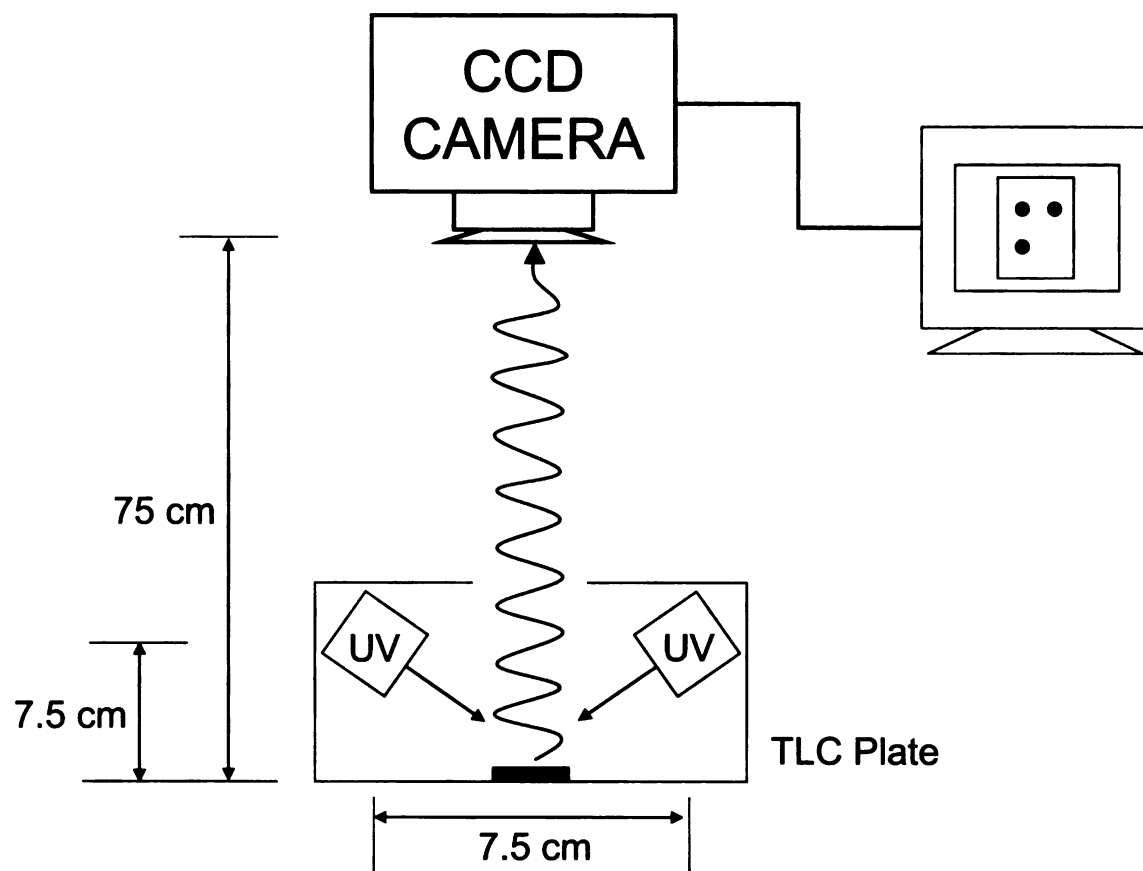


**Figure 3.1.** Diagram of TLC plate imaging setup.

distance and angle between the lamp and the plate. The greatest fluorescence power was observed when the lamp was placed directly above and parallel to the plate. Because this orientation was not possible for imaging, two UV lamps were used to provide illumination from both sides of the TLC plate.

For positional reproducibility, the TLC plate was placed on a grid that was fixed to the bench top. The two lamps were secured 7.5 cm above the plate at  $\sim 30^\circ$  to the surface with a 7.5 cm separation between the two lamps. In addition, the UV lamps required one hour of stabilization to obtain a constant fluorescence power of the TLC plate, as shown in Figure 3.2. The stabilization time was a result of fluctuation in the lamp output, not in the degradation of the fluorophore or stationary phase. The lens of the CCD camera was positioned approximately 75 cm from the plate and the position was fixed by using a locking clamp. This height was sufficient to image the entire plate with appropriate resolution. To reduce extraneous light that may result in increased noise, all images were acquired in the absence of natural or ambient light.

### **3.2 Optimization of Image Acquisition and Manipulation**

Grayscale images were collected by using V for Windows software (Version 3.5, Photometrics, Tuscon, AZ), which controlled exposure time of the camera as well as manipulation of the image for extraction of chemical data. To correct for the dark current of the CCD camera, a bias image, acquired with the shutter closed, was subtracted from every image. As described by Simon and coworkers,<sup>1</sup> the intensities of the sample plates were also corrected for illumination gradients using intensities from a background image that does not

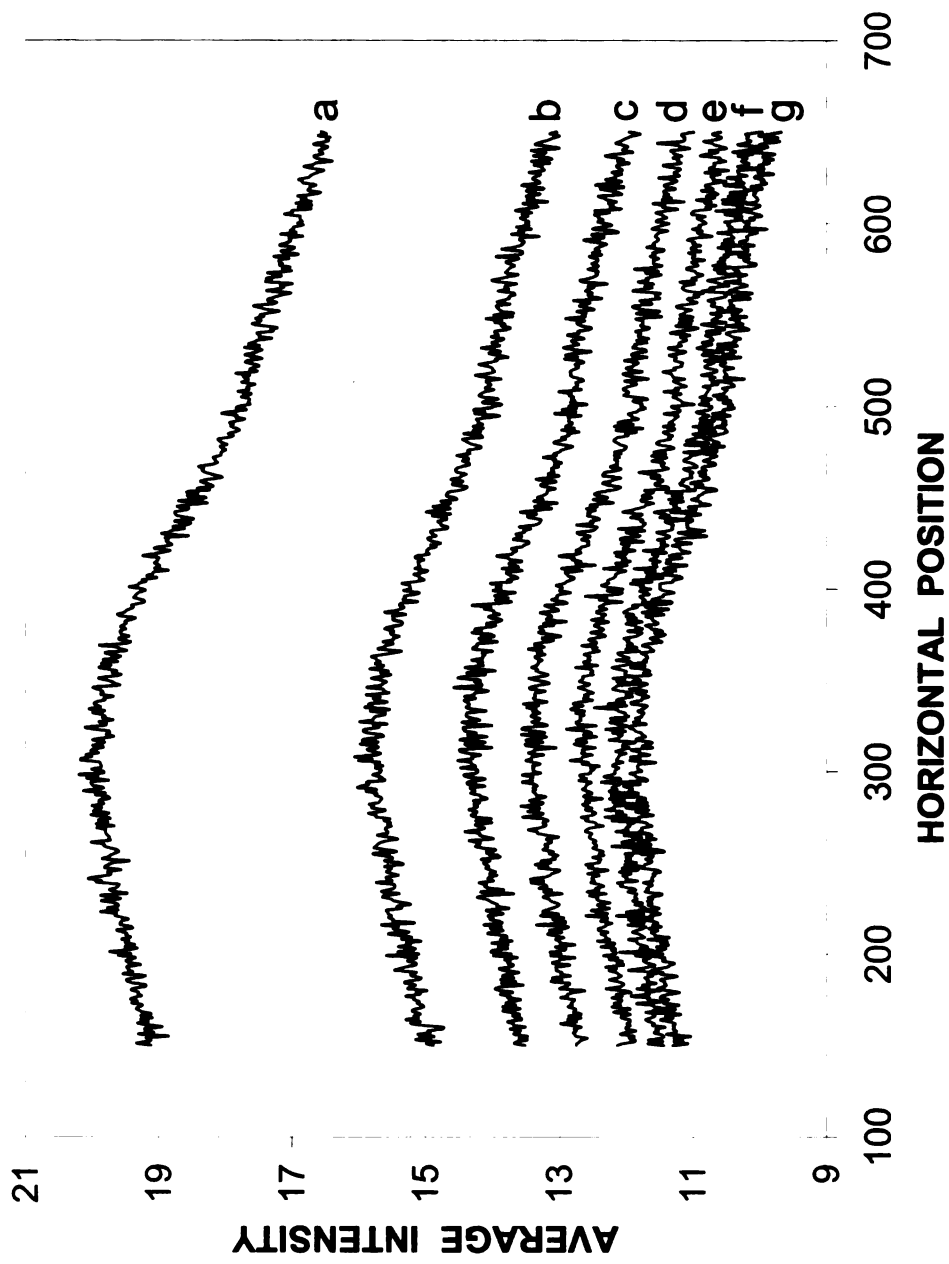


**Figure 3.2.** Fluorescence of a TLC plate at various times after turning on the UV lamp: (a) 5 min, (b) 15 min, (c) 25 min, (d) 35 min, (e) 45 min, (f) 55 min, (g) 65 min.

contain the solutes of interest, as described by Equation 3.1.

$$\text{Corrected Intensity} = \frac{\text{Raw Intensity}}{\text{Background Intensity}} \times \text{Average Background Value} \quad (3.1)$$

Corrected intensity values were plotted versus horizontal pixel position to result in a peak at the location of the solute zone (Figure 3.3). This area has an increased signal, or ratio of intensities of the sample and background plates, above the background level, and the center of the zone corresponds to the peak maximum. The peak height represents the mass at the center of the zone, while the peak area represents the mass of the entire zone.

Prior to image acquisition, values for gain and integration time are selected by the operator. Gain is commonly used to describe the electronic amplification of a signal, where a greater value for gain implies a greater amplification.<sup>2</sup> To examine the effect of gain in this experimental system, images of TLC plates were collected before and after application of 3.6  $\mu\text{g}$  of NB at gain levels 1, 2, and 3 using an integration time of 500 ms. The signal-to-noise and signal-to-background ratios were compared for the corrected images to determine the optimum gain setting (Table 3.1). The signal-to-noise (S/N) ratio was constant and the signal-to-background (S/B) ratio decreased when the gain was increased. The decrease in S/B ratio resulted in decreased peak height and area at higher gain levels. All subsequent images were obtained using gain level 1 to ensure maximum peak heights and areas were calculated.

An integration time is also specified by the operator prior to image acquisition. The integration time describes the time that the shutter is exposed to

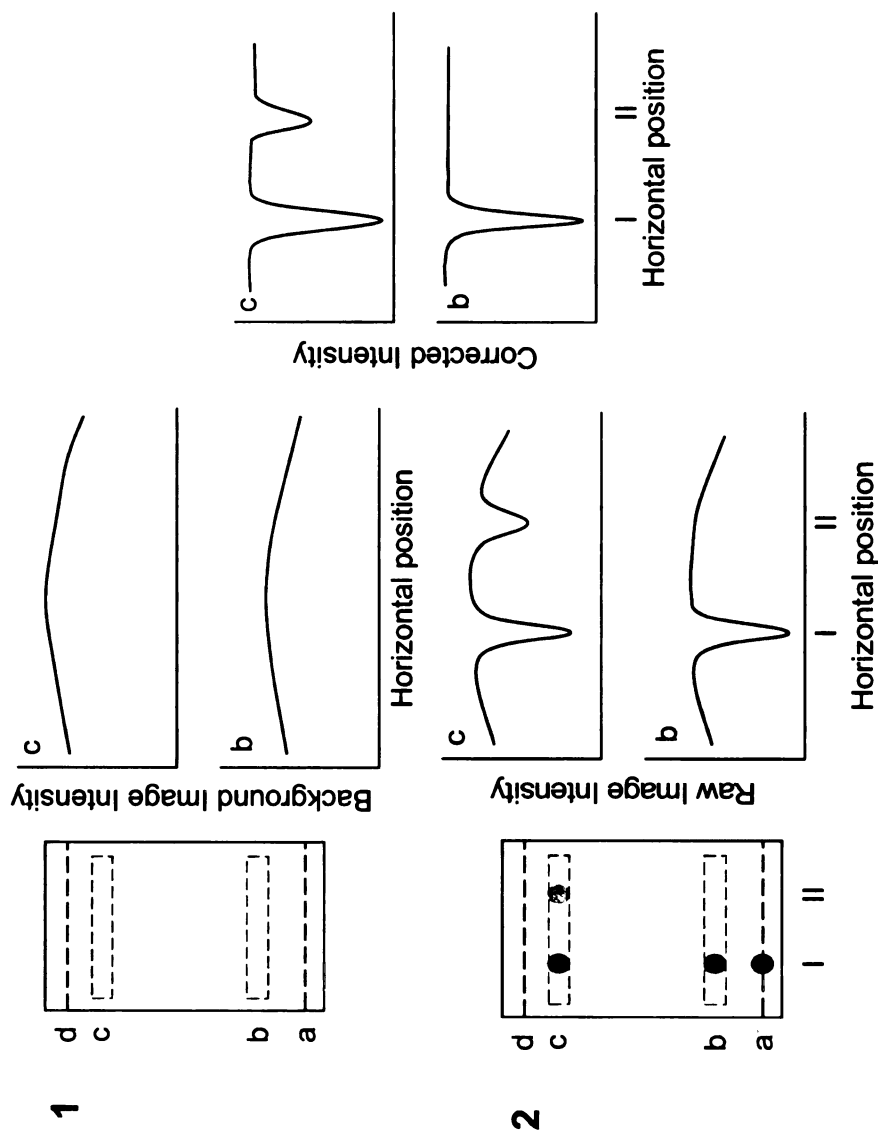


**Figure 3.3.** Simulated images and chromatograms for (1) a background plate and (2) a sample plate containing (I) a reference sample and (II) an unknown sample. Designated plate areas include (a) the original location and a completely retained solute, (b) the binning area around a strongly retained solute that is undetected in the unknown sample and the corresponding chromatogram, (c) the binning area around a weakly retained solute detected in both samples but at different concentrations and the corresponding chromatogram, and (d) the solvent front. The corrected intensity is calculated by using Equation 3.1.

**Table 3.1.** Comparison of image quality for various gain settings obtained with an integration time of 500 ms.

<b>Gain Level</b>	<b>1</b>	<b>2</b>	<b>3</b>
Signal (S)	0.0799	0.0501	0.0346
Noise (N)	0.0173	0.0119	0.00736
Background (B)	1.01	0.999	0.987
S/N Ratio	4.62	4.21	4.70
S/B Ratio	0.0793	0.0501	0.0351

the illuminated plate, where long integration times generally result in higher signals. At significantly large integration times, however, overexposure may occur, resulting in decreased pixel resolution. To determine the optimum integration time, images of TLC plates were collected before and after application of 3.6  $\mu\text{g}$  of NB at integration times from 100 to 4000 ms. The S/N and S/B ratios were compared for the corrected images (Table 3.2). Because the signal corresponds to a ratio of the sample to the background intensity (Equation 3.1), the signal and background did not increase with increasing integration time. An increase in both the S/N and S/B ratios was observed with increasing integration time. Although the S/B decreased slightly at integration times greater than 1000 ms, this decrease was considered acceptable relative to the greater gain in S/N ratio. Based on this study, an integration time of 4000 ms was utilized for all subsequent measurements.

The V for Windows software also allows selection of a portion of the image for further numerical analysis. Once the selection was made, pixel values could be summed or averaged in the horizontal or vertical direction. For TLC plate images, the horizontal direction was perpendicular to the solvent flow, while the vertical direction was parallel to the solvent flow (Figure 3.3). Because the solute zones traveled with the solvent in the horizontal direction, the mathematical operation was performed in that direction to be meaningful. For both summing and averaging of the pixel values, the amount of fluorescent background included in the selection was also important. The program assigned the greatest values to illuminated pixels and lesser values for darker areas. Because the solute zones

**Table 3.2.** Comparison of image quality for various integration times.

<b>Integration Time (ms)</b>	<b>100</b>	<b>500</b>	<b>1000</b>	<b>2000</b>	<b>3000</b>	<b>4000</b>
Signal (S)	0.0863	0.0903	0.0914	0.0869	0.0836	0.0815
Noise (N)	0.168	0.0145	0.00755	0.00508	0.00474	0.00366
Background (B)	1.78	1.01	0.9987	0.994	1.00	0.997
S/N Ratio	0.513	6.25	12.1	17.1	17.6	22.3
S/B Ratio	0.0485	0.0892	0.0916	0.0874	0.0835	0.0818

appeared dark, the assigned pixel values were low in these areas. Incorporation of background fluorescence into the sum or average around the zone therefore resulted in higher backgrounds without an increase in signal. To compare the effect of summing and averaging of pixels, images of TLC plates were collected before and after application of 3.6  $\mu\text{g}$  of NB. The S/N and S/B ratios were compared for selections of various heights of the corrected images (Table 3.3). Overall, signal summing and averaging resulted in comparable S/N and S/B ratios. Increasing the size of the selection, however, decreased both the S/N and S/B ratios, because more fluorescence background was incorporated into the larger selection. Based on this observation, all selections in subsequent measurements were chosen around the solute zone to minimize fluorescence background inclusion. Although summing and averaging resulted in similar figures of merit, summation was chosen for subsequent measurements. Because mass diffuses radially from the center of each solute zone throughout the development process, the areas near the edge will contain less mass and therefore appear lighter in the image. Summation of the pixels will not discount the lighter areas of less mass, and will therefore be more physically meaningful.

### **3.3 Correction Using a Background Plate**

As described by Equation 3.1, raw images were corrected using the fluorescence of a background TLC plate that did not contain the solutes of interest. The best method for background correction would be to acquire an image of the same plate before and after chromatographic development. In the field, however, this approach would be time consuming and impractical. To

**Table 3.3.** Comparison of image quality for summing and averaging pixels in different size selections of the image.

Selection Height (pixels)	Sum of Pixels			Average of Pixels		
	143	221	306	143	221	306
Signal (S)	0.0233	0.0177	0.0127	0.0352	0.0217	0.0137
Noise (N)	0.00208	0.00186	0.00183	0.00313	0.00227	0.00199
Background (B)	0.731	0.890	0.994	1.10	1.09	1.08
S/N Ratio	11.2	9.51	6.92	11.3	9.58	6.89
S/B Ratio	0.0318	0.0199	0.0127	0.0320	0.0200	0.0127

determine if different plates could be used for the background and sample images, several situations were considered. First, repeat measurements of the same plate were conducted in which the plate was removed from the imaging location between acquisitions. The RSD of the background fluorescence for repeat measurements of the same plate was less than 5% when the dimensions of the summation area were consistent between images. The fluorescence of several TLC plates from the same lot was similarly compared, with an RSD of less than 5%. The fluorescence of several TLC plates from the same lot was also compared for orientations relative to the direction that the solvent traveled during the washing step. The orientation of the plate did not affect the measured fluorescence, with an RSD less than 5%. Because the fluorescence of background plates was consistent, a single background plate can be used for all image corrections within that lot. The background image must be acquired at the same time as the sample image, however, to provide a consistent illumination profile and appropriate background correction. Similarly, the selection from the background plate must be from the same location as the selection from the sample plate. In addition, the background and sample plates must be pretreated in methanol at a similar time to ensure consistent fluorescence emission.

### **3.4 Theory and Data Analysis**

Peak heights and areas were determined by visual inspection in Microsoft Excel as well as through the use of computer software (PeakFit, version 3.18, SYSTAT Software, San Jose, CA). Because mass diffuses radially from the center of the zone during the chromatographic process, peak area represents the

entire mass of the sample. Conversely, the peak height represents the mass only at the center of the zone, and although it can be used for quantitation, peak height is less representative of the entire sample. For peak height, manual determination in Microsoft Excel was accomplished by subtracting the average baseline level from the maximum intensity value. For peak area, a right Riemann sum was used to approximate the integration, as described by Equation 3.2

$$\sum_{i=1}^n y_i (x_i - x_{i-1}) \quad (3.2)$$

x and y are the coordinates of each point being integrated. A Riemann sum calculated from the average baseline level was subtracted from the Riemann sum of the solute zone to normalize all baselines to zero.

Peak heights and areas were also determined by fitting to a symmetric double-sigmoidal function using PeakFit software, as shown in Equation 3.3

$$\frac{I}{I_0} = \frac{a}{1 + \exp\left[-\left(\frac{x - b + \frac{c}{2}}{d}\right)\right]} \left[ 1 - \frac{1}{1 + \exp\left[-\left(\frac{x - b - \frac{c}{2}}{d}\right)\right]} \right] \quad (3.3)$$

where x is horizontal position. The symmetric double-sigmoidal function was determined to best represent the shape of the solute zones through iterative determination of constants a, b, c, and d. Figure 3.4 demonstrates the quality of fit generated by the PeakFit program. The PeakFit program also incorporated the shape of the baseline in the generated function, and the best fit equation was used to determine peak height and area. In general, a more accurate representation of the peak height and area was obtained by using PeakFit and

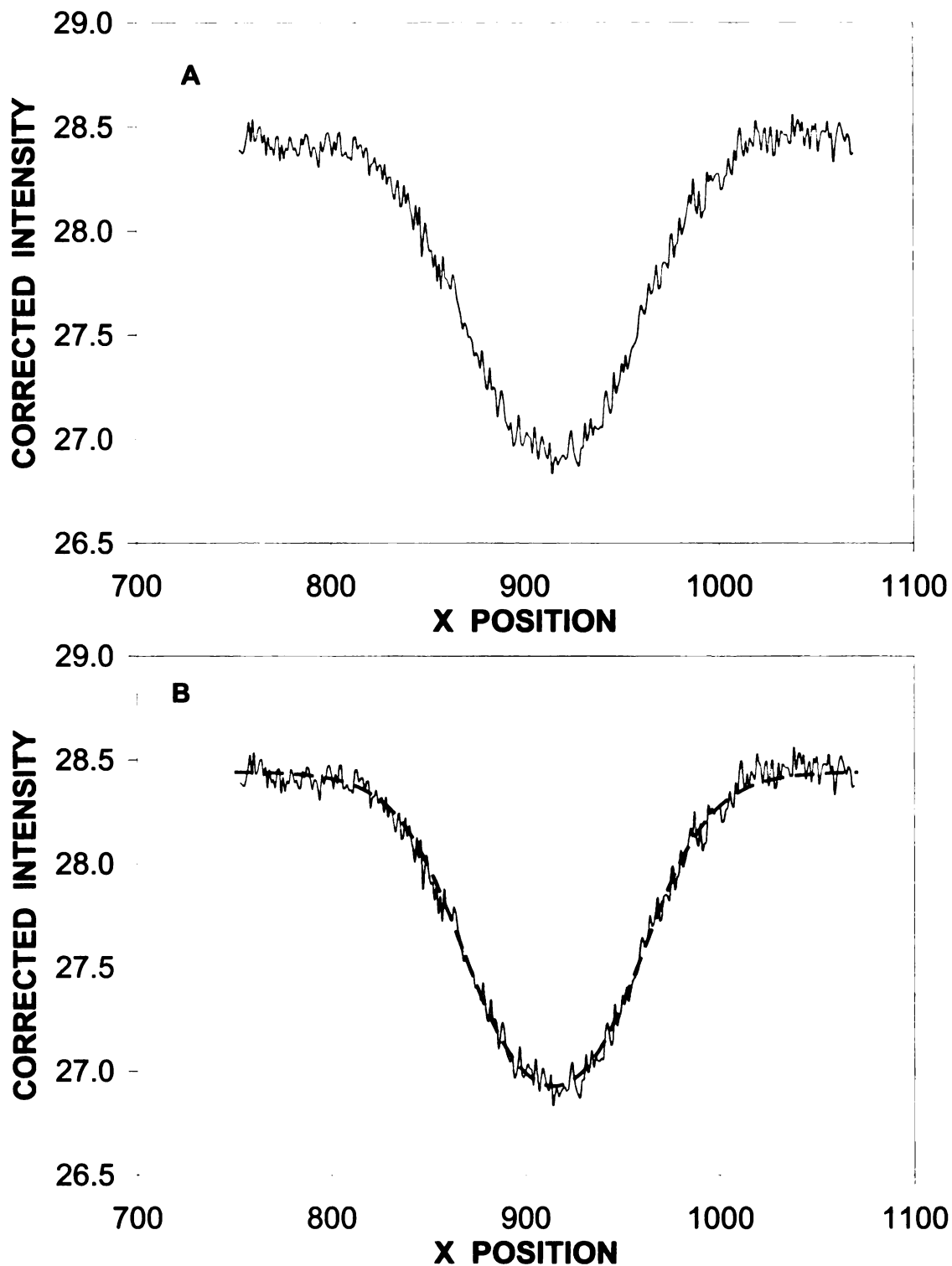


**Figure 3.4.** Fit of TNT to the symmetric double-sigmoidal function (Equation 3.3). (A) Corrected intensity for 9.8  $\mu\text{g}$  TNT. (B) Symmetric double-sigmoidal fit of 9.8  $\mu\text{g}$  TNT data (— — —),  $R^2 = 0.987$ .

therefore all reported values were determined with this method.

Using both the peak height and area, calibration curves were constructed for each of the solutes. At low concentrations, a semi-logarithmic relationship is predicted by Beer's Law, as shown in Equation 3.4

$$A = -\log\left(\frac{I}{I_0}\right) = \epsilon bc \quad (3.4)$$

As traditionally defined, A is the absorbance,  $\epsilon$  is the molar absorptivity, b is the pathlength, and c is the concentration. I is the intensity after sample interaction, and  $I_0$  is the intensity of the source light. For this application, the corrected image is a ratio of the intensity of the sample plate (I) to the intensity of the background plate ( $I_0$ ) according to Equation 3.1, and is therefore analogous to the intensity ratio ( $I/I_0$ ) in Equation 3.4. In addition, the concentration (c) is related to the mass of the sample, as the solvent was evaporated prior to the measurement. As a result, Beer's Law predicts that the mass of the sample is linear with the logarithm of the peak height or area. This relationship was observed by Simon and coworkers for a variety of organic pharmaceuticals.<sup>3,4</sup>

The underlying assumptions of Beer's Law require that the solute be low in concentration and be distributed randomly throughout the medium. On a TLC plate, however, as the concentration of molecules increases, solute molecules may arrange non-randomly to maximize the interaction between them as the solvent evaporates. The process of solute application onto the plate may also result in layering of the molecules, which can in turn affect uniformity. In order to extend the linear range to higher masses, an empirical equation (Equation 3.5)

was identified to describe the nonlinear relationship between mass (m) and the logarithm of peak height or area (I/I<sub>0</sub>).

$$\log \left( \frac{I}{I_0} \right) = w + z \log m \quad (3.5)$$

Using this equation, the logarithm of the peak height or area was linearly related to the logarithm of the concentration. Detection limits were calculated based on peak height data using both relationships (Equations 3.4 and 3.5) as the theoretical concentration that would yield a S/N ratio of 4.353 at the 90% confidence level.<sup>1,5-7</sup> Linear ranges for each of the explosives and degradation products were taken as the mass range extending from the detection limit to the maximum concentration used in this study. The detection limits and linear ranges determined for each class of explosives is discussed in the following sections.

### **3.5 Quantitation of Degradation Products**

At low concentrations, calibration curves were calculated using Equation 3.4 and are shown in Figures 3.5A-3.9A for each of the degradation products. For the entire concentration range, calibration curves were calculated using Equation 3.5 and are shown in Figures 3.5B-3.9B. Similar trends were observed when curves were calculated based on peak height and area, and only the results for peak area are shown here. Table 3.4 summarizes the correlation coefficients for the semi-logarithmic fits (Equation 3.4) of both the peak height and area data for each of the solutes. Table 3.5 summarizes the correlation coefficients for the logarithmic fits (Equation 3.5) of both the peak height and

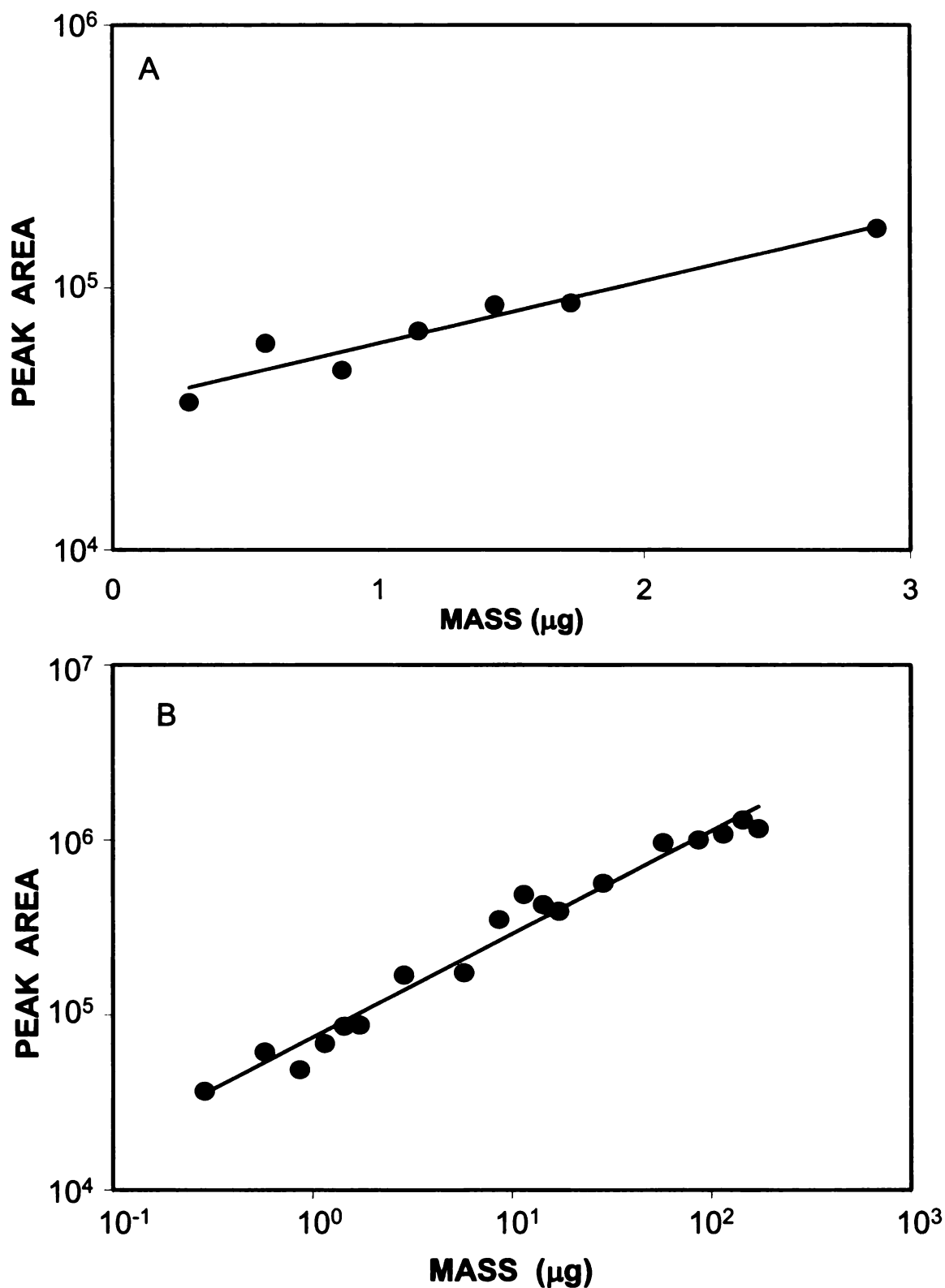


**Figure 3.5.** Calibration curves for NB based on peak area using (A) the semi-logarithmic fit described in Equation 3.4 and (B) the logarithmic fit described in Equation 3.5.

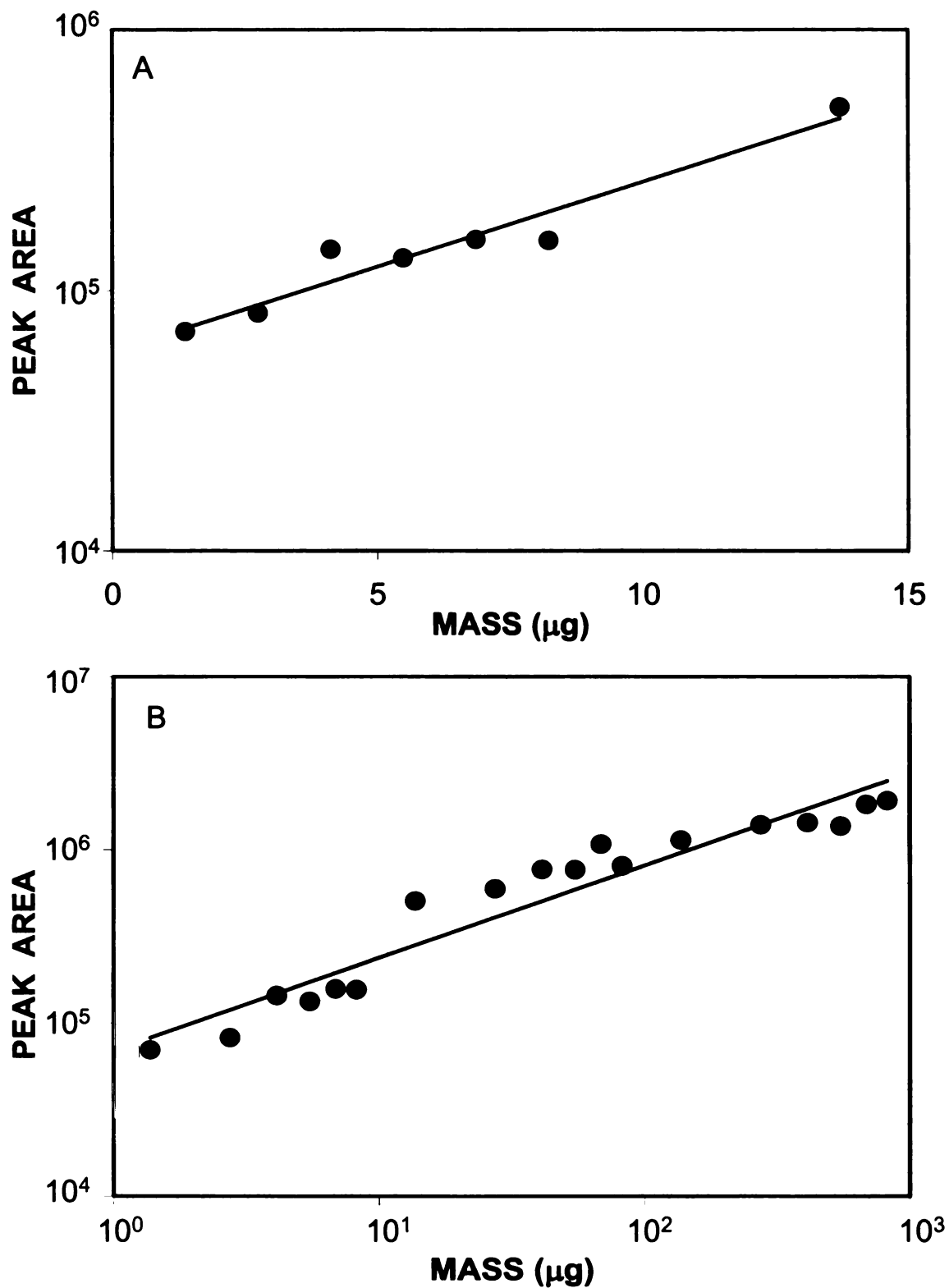


**Figure 3.6.** Calibration curves for 2-NT based on peak area using (A) the semi-logarithmic fit described in Equation 3.4 and (B) the logarithmic fit described in Equation 3.5.

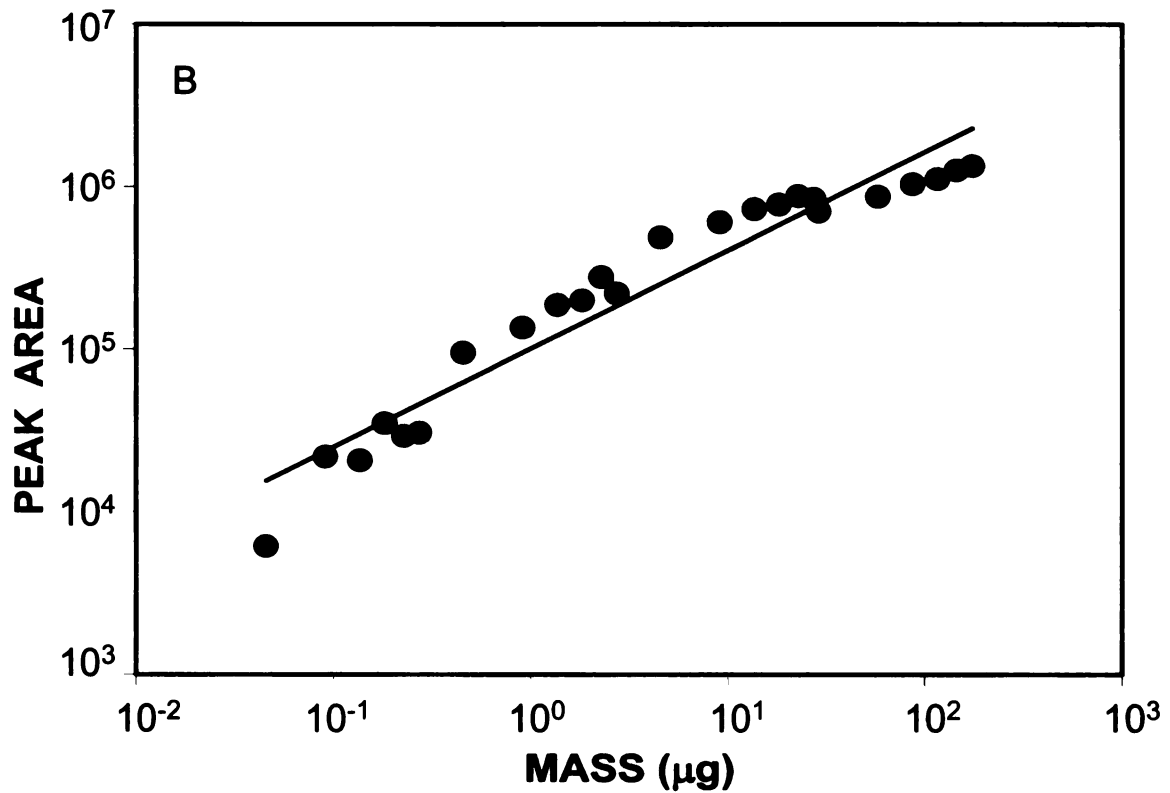
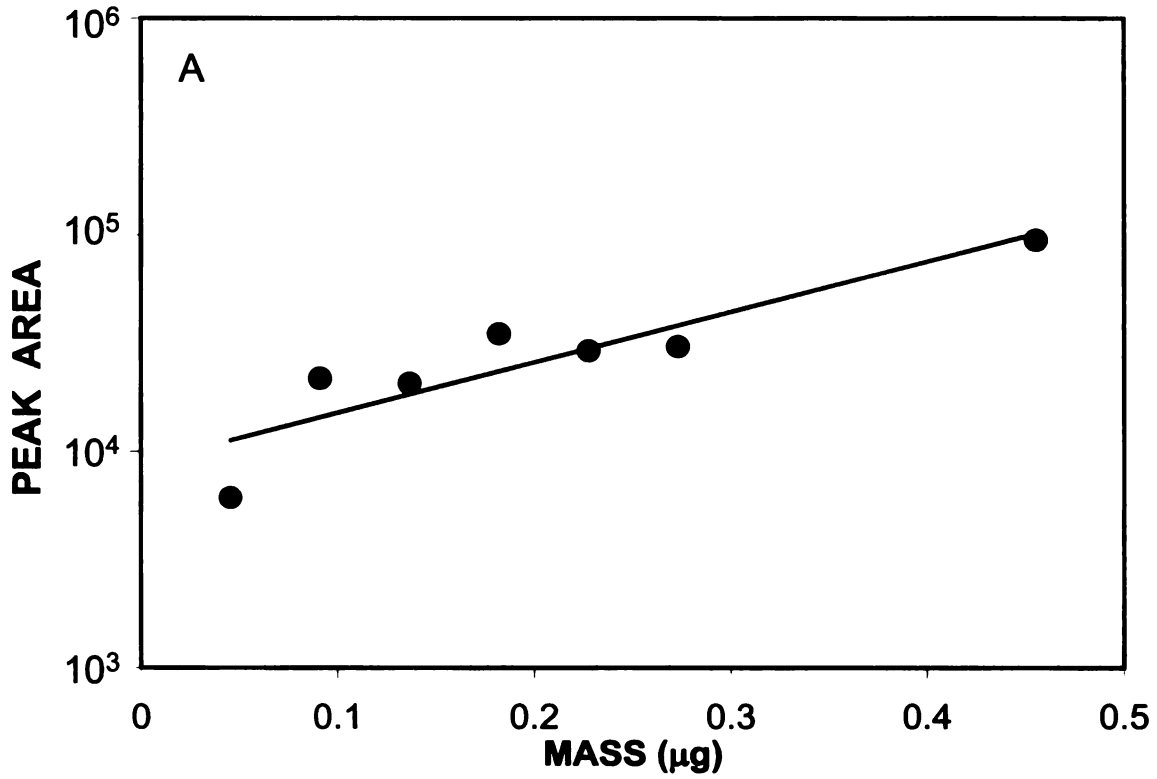


**Figure 3.7.** Calibration curves for 2,4-DNT based on peak area using (A) the semi-logarithmic fit described in Equation 3.4 and (B) the logarithmic fit described in Equation 3.5.

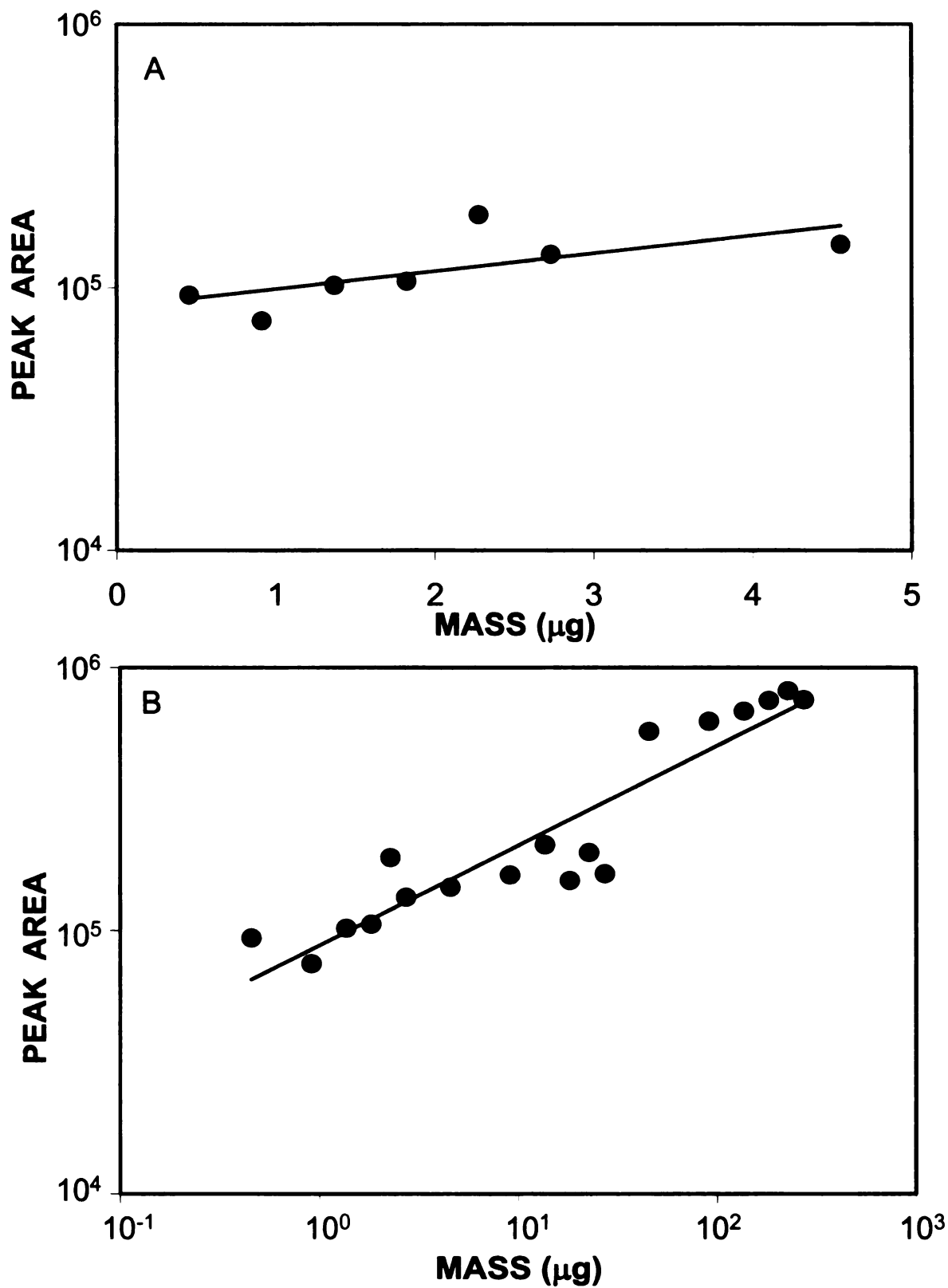


**Figure 3.8.** Calibration curves for 2,6-DNT based on peak area using (A) the semi-logarithmic fit described in Equation 3.4 and (B) the logarithmic fit described in Equation 3.5.

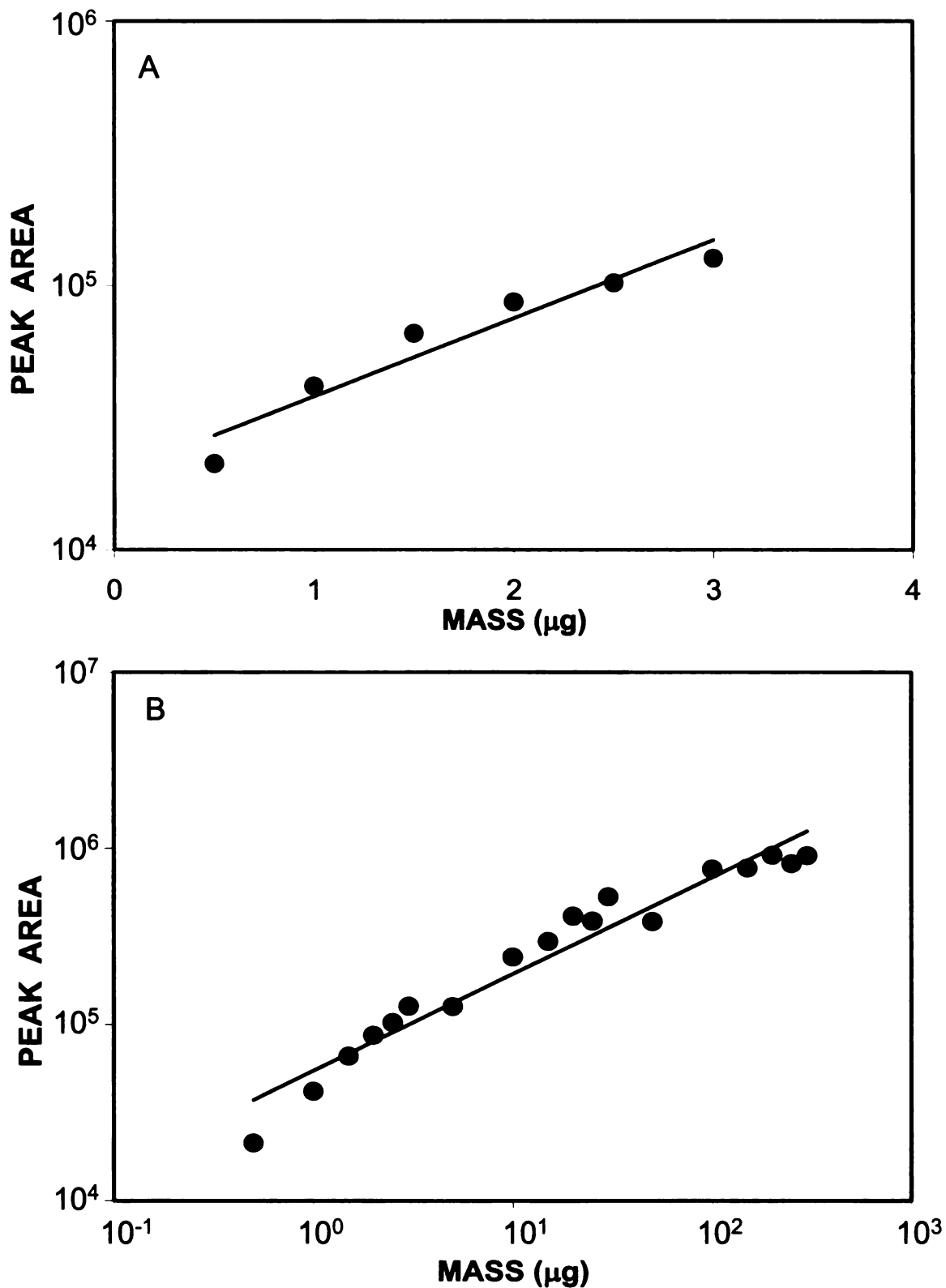


**Figure 3.9.** Calibration curves for 4-am-DNT based on peak area using (A) the semi-logarithmic fit described in Equation 3.4 and (B) the logarithmic fit described in Equation 3.5.

**Table 3.4.** Detection figures of merit for nitrated explosives and degradation products using the semi-logarithmic function (Equation 3.4).

Nitrated Explosive	Correlation Coefficient ( $R^2$ )		Limit of Detection ( $\mu\text{g}$ ) <sup>a</sup>	Linear Range ( $\mu\text{g}$ )
	Peak Height	Peak Area		
NB	0.9807	0.9245	1.5 ± 0.1	0.3 – 2.8
2-NT	0.9305	0.9325	NA <sup>b</sup>	1.4 – 14
2,4-DNT	0.9075	0.8061	0.35 ± 0.06	0.05 – 0.46
2,6-DNT	0.5166	0.4691	NA	0.5 – 4.6
4-am-DNT	0.9283	0.9274	0.4 ± 0.3	0.5 – 3
TNT	0.7517	0.7615	3 ± 1	0.2 – 6
Tetryl	0.7536	0.6775	5 ± 1	0.4 – 5
Picric acid	0.8538	0.9159	NA	0.07 – 1.4
RDX	0.3751	0.5002	5 ± 4	0.5 – 4.8
HMX	0.4071	0.0282	NA	0.3 – 1.8
NG	0.0085	0.0051	NA	55 – 330
PETN	0.5721	0.0471	NA	63 – 250

<sup>a</sup> Determined using  $S/N = 4.353$ .

<sup>b</sup> NA = not available. Value determined to be negative from poor linear correlation.

**Table 3.5.** Detection figures of merit for nitrated explosives and degradation products using the logarithmic function (Equation 3.5).

Nitrated Explosive	Correlation Coefficient ( $R^2$ )		Limit of Detection ( $\mu\text{g}$ ) <sup>a</sup>	Linear Range ( $\mu\text{g}$ )
	Peak Height	Peak Area		
NB	0.9515	0.9722	1.2 ± 0.2	1.2 – 170
2-NT	0.8765	0.9222	0.16 ± 0.07	1.4 – 820
2,4-DNT	0.9103	0.9303	0.38 ± 0.08	0.4 – 170
2,6-DNT	0.8429	0.8649	0.14 ± 0.06	0.5 – 270
4-am-DNT	0.9367	0.9469	0.30 ± 0.07	0.5 – 300
TNT	0.9372	0.9444	2.4 ± 0.4	2.4– 420
Tetryl	0.9415	0.9086	6 ± 1	6 – 190
Picric acid	0.9631	0.9841	0.040 ± 0.007	0.07 – 41
RDX	0.8725	0.8939	5 ± 2	5 – 360
HMX	0.8803	0.9187	6 ± 2	6 – 200
NG	0.0705	0.0432	1 ± 4	55 – 330
PETN	0.5077	0.0144	10 ± 10	63 – 250

<sup>a</sup> Determined using S/N = 4.353.

area data for each of the solutes. The correlation coefficients, or  $R^2$  values, represent the quality of fit between the data and the mathematical relationship of interest. Correlation coefficients can vary between zero and unity, with a value of zero indicating no correlation and a value of unity indicating a perfect correlation.

For most of the degradation products, the logarithmic expression over the entire concentration range (Equation 3.5) was a better fit to the data than the semi-logarithmic expression at low concentration (Equation 3.4), as seen from the correlation coefficients (Tables 3.4 and 3.5). The semi-logarithmic correlation coefficients for NB, 2-NT, and 4-am-DNT were greater than 0.9, indicating a reasonable fit for these solutes in the low concentration range. The semi-logarithmic correlation coefficients for 2,4-DNT and 2,6-DNT, however, were significantly less, and the lower quality of fit is evident in Figures 3.7A and 3.8A. The quality of fit was improved significantly by using the logarithmic expression for all of the degradation products except 2-NT, for which the fit was slightly poorer for the logarithmic expression. Despite the decrease in fit quality, the correlation coefficient for 2-NT was greater than 0.9. Using the logarithmic fit, the linear ranges were extended to three orders of magnitude, compared with one order of magnitude for the semi-logarithmic fit. By considering only the linear range of the two mathematical fits, the logarithmic fit will be much more useful in the analysis of a sample of unknown concentration.

Detection limits were also calculated for each of the degradation products using both the semi-logarithmic (Table 3.4) and logarithmic (Table 3.5) fits of peak height data. For many of the degradation products, the semi-logarithmic fit

was so poor that the calculated detection limits were negative and were therefore not meaningful. Detection limits calculated for NB, 2,4-DNT, and 4-am-DNT and were in the low  $\mu\text{g}$  range. Using the logarithmic fit, however, detection limits for all degradation products were in the low  $\mu\text{g}$  range. The detection limits for NB, 2,4-DNT, 4-am-DNT calculated by using the logarithmic function were comparable to those calculated by using the semi-logarithmic function, and were comparable to those reported for nitroaromatic explosives using densitometry.<sup>8,9</sup>

### **3.6 Quantitation of Nitroaromatic Explosives**

For quantitation, tetryl was classified with nitroaromatic explosives despite its nitramine character, as the aromatic character was most important in the absorption-based quantitation process. Calibration curves were calculated using Equations 3.4 and 3.5 and are shown in Figures 3.10-3.12 for TNT, tetryl, and picric acid, respectively. Again, because curves for peak height and area followed the same trend, only peak area curves are shown. Tables 3.4 and 3.5 summarize the correlation coefficients for the semi-logarithmic and logarithmic fits of the data, respectively.

For TNT, tetryl, and picric acid, the logarithmic expression over the entire concentration range (Equation 3.5) was a better fit to the data than the semi-logarithmic expression at low concentration (Equation 3.4), as seen from the correlation coefficients (Tables 3.4 and 3.5). The quality of fit for the semi-logarithmic expression was acceptable for picric acid, with a correlation coefficient greater than 0.9. The regressions for TNT and tetryl were less satisfactory, as seen from Figures 3.10A and 3.11A. As observed with the

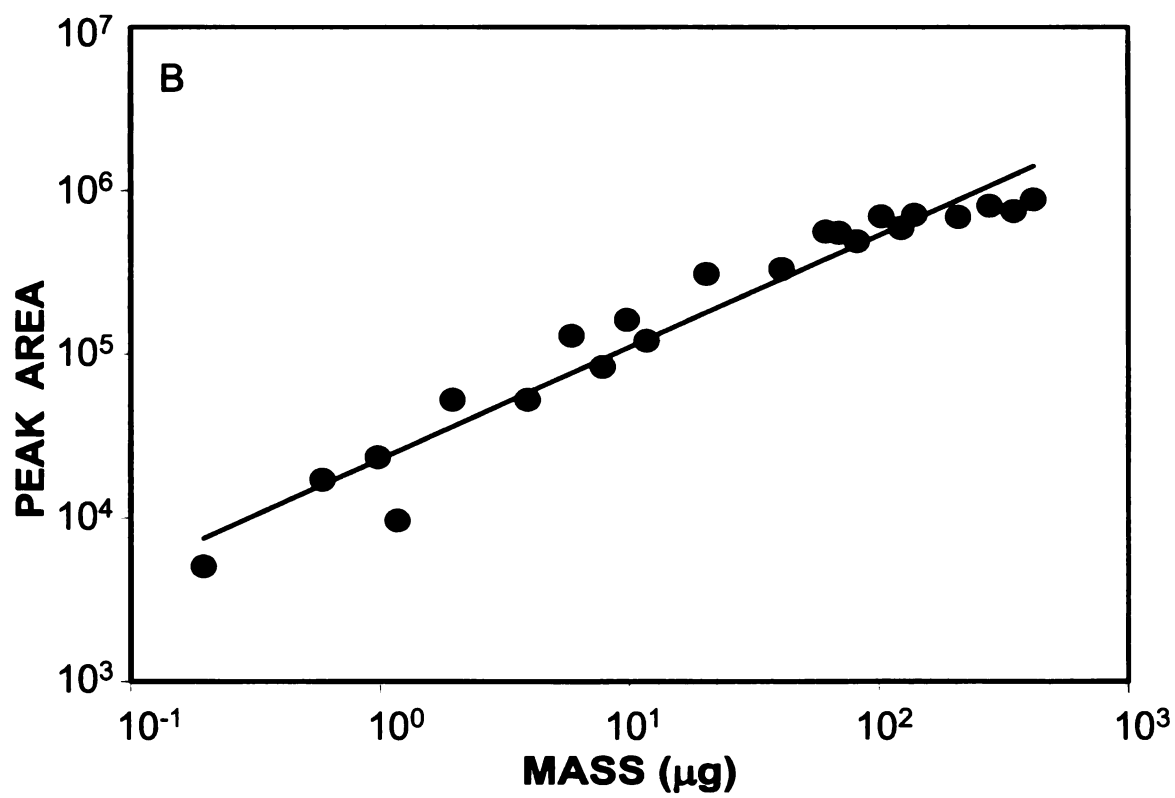
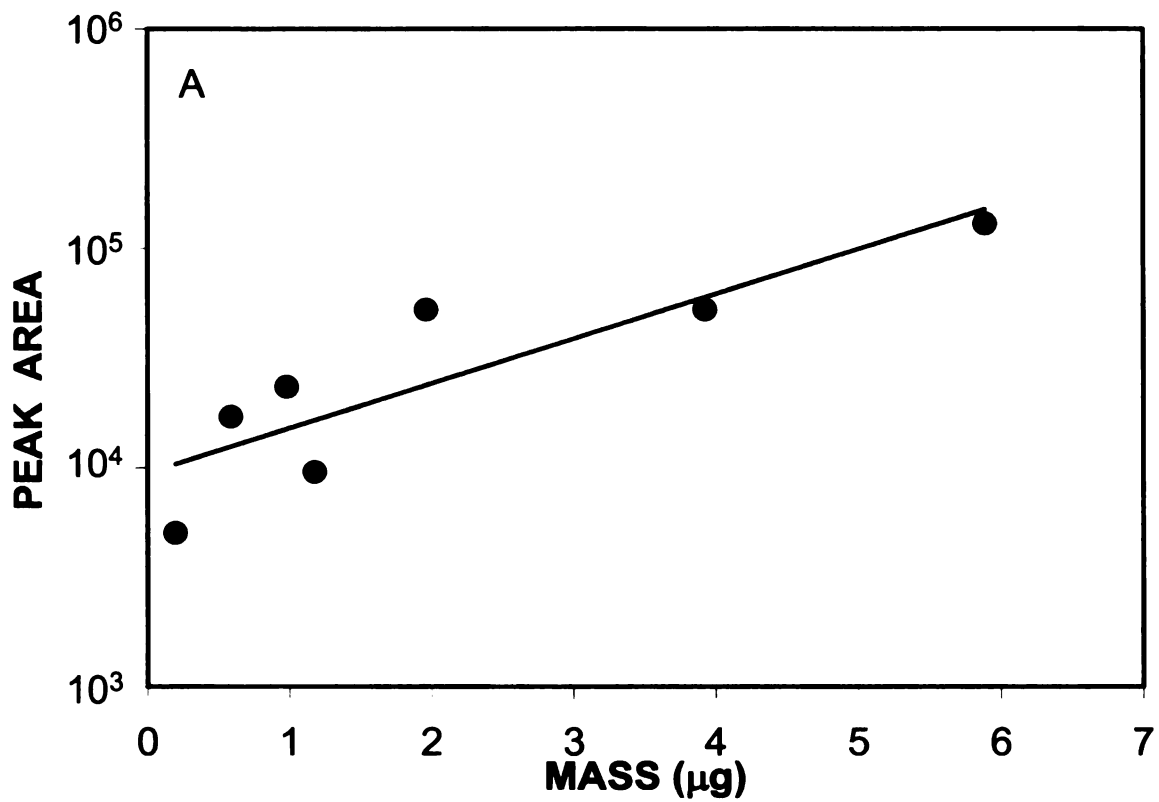


**Figure 3.10.** Calibration curves for TNT based on peak area using (A) the semi-logarithmic fit described in Equation 3.4 and (B) the logarithmic fit described in Equation 3.5.

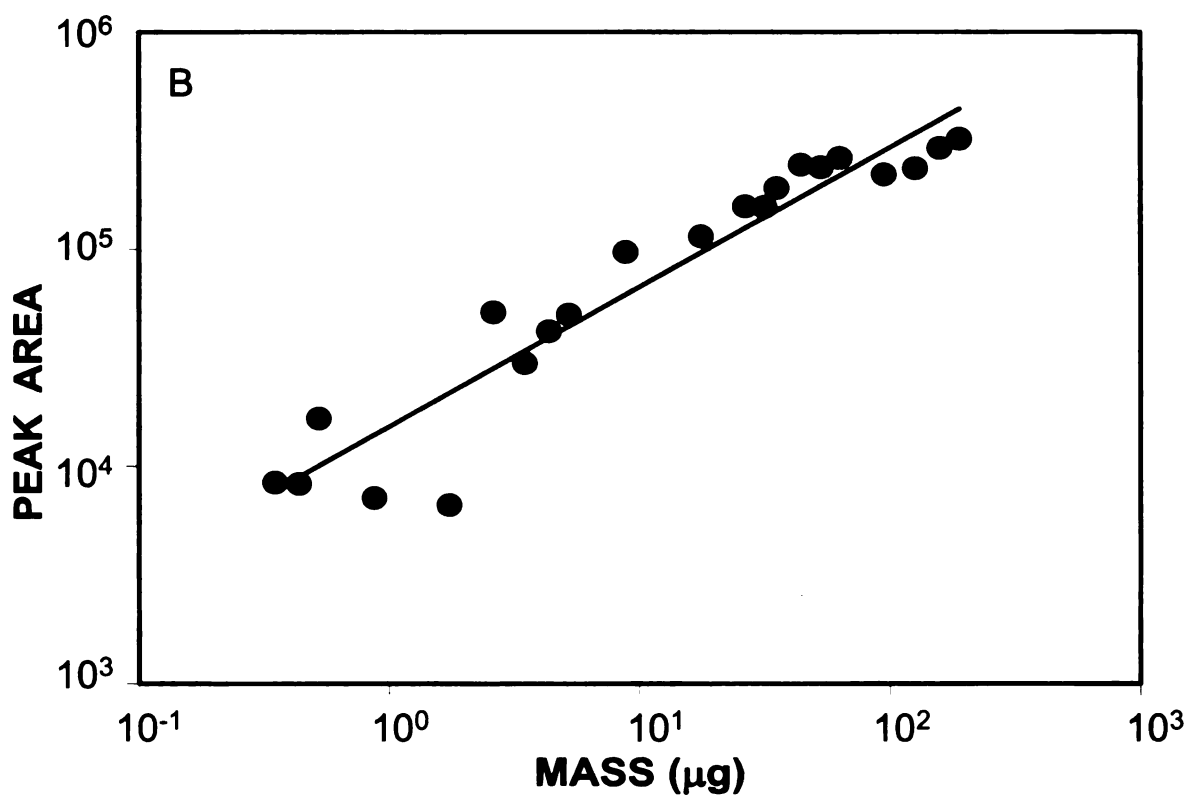
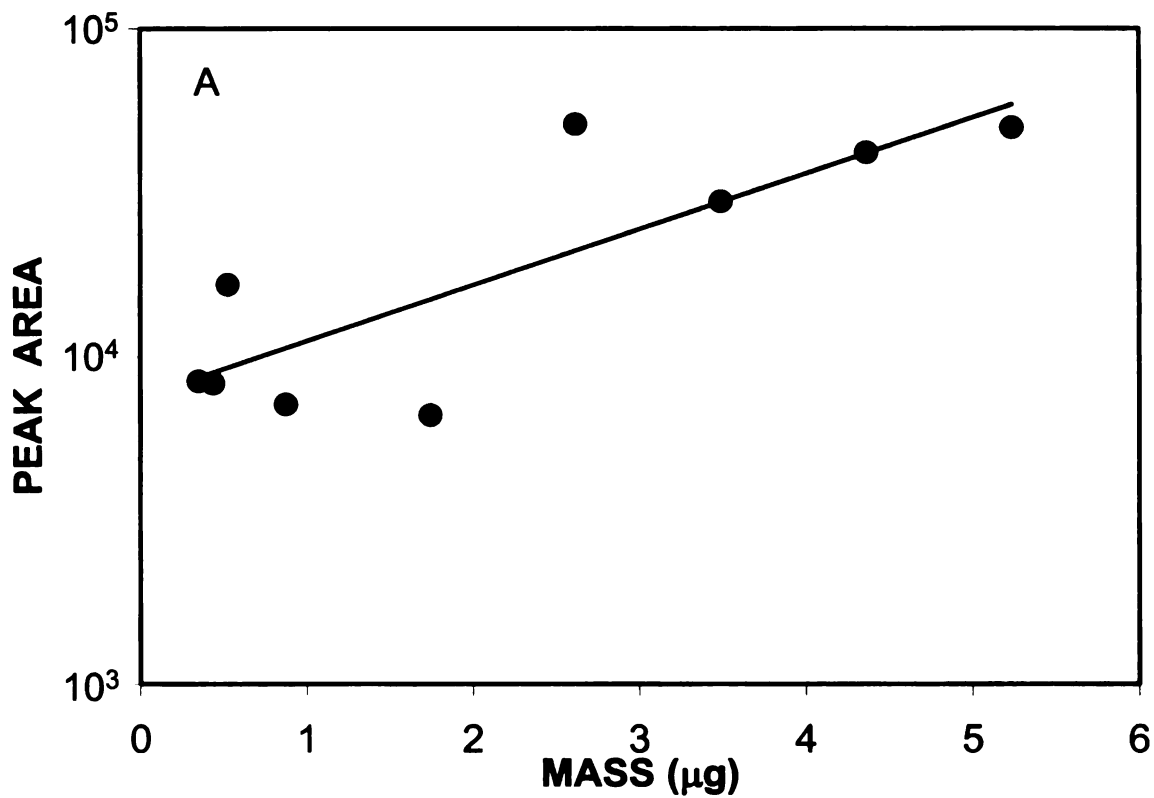


**Figure 3.11.** Calibration curves for tetryl based on peak area using (A) the semi-logarithmic fit described in Equation 3.4 and (B) the logarithmic fit described in Equation 3.5.

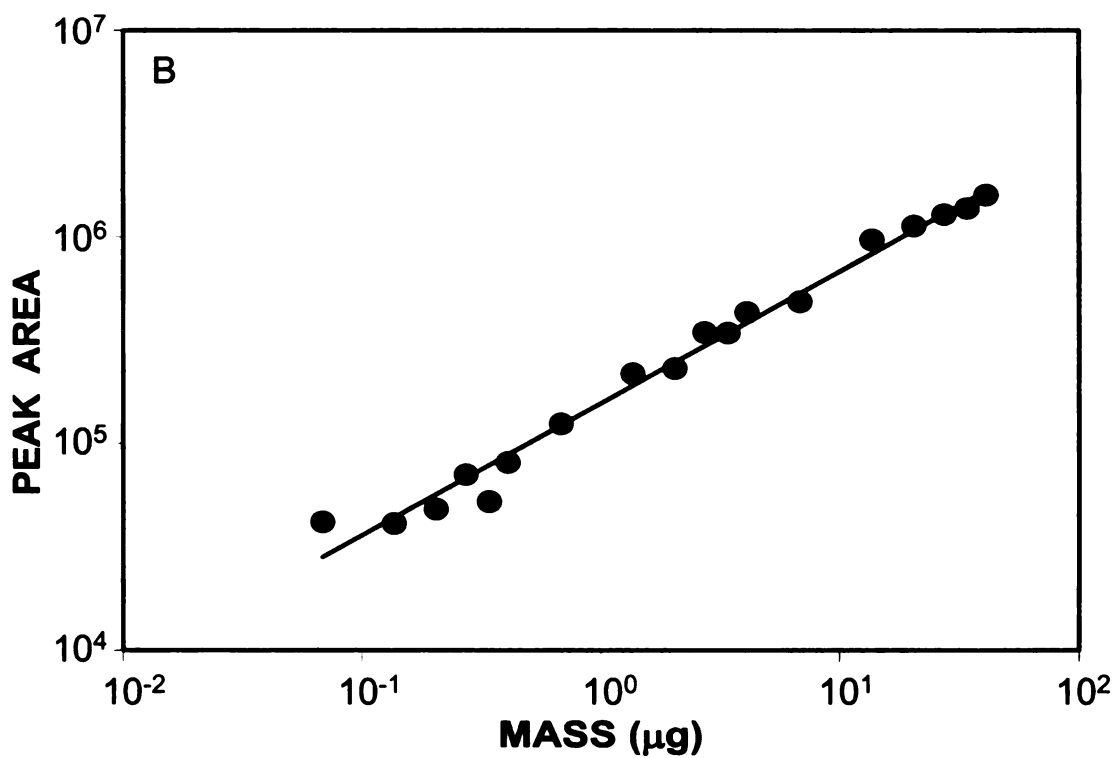
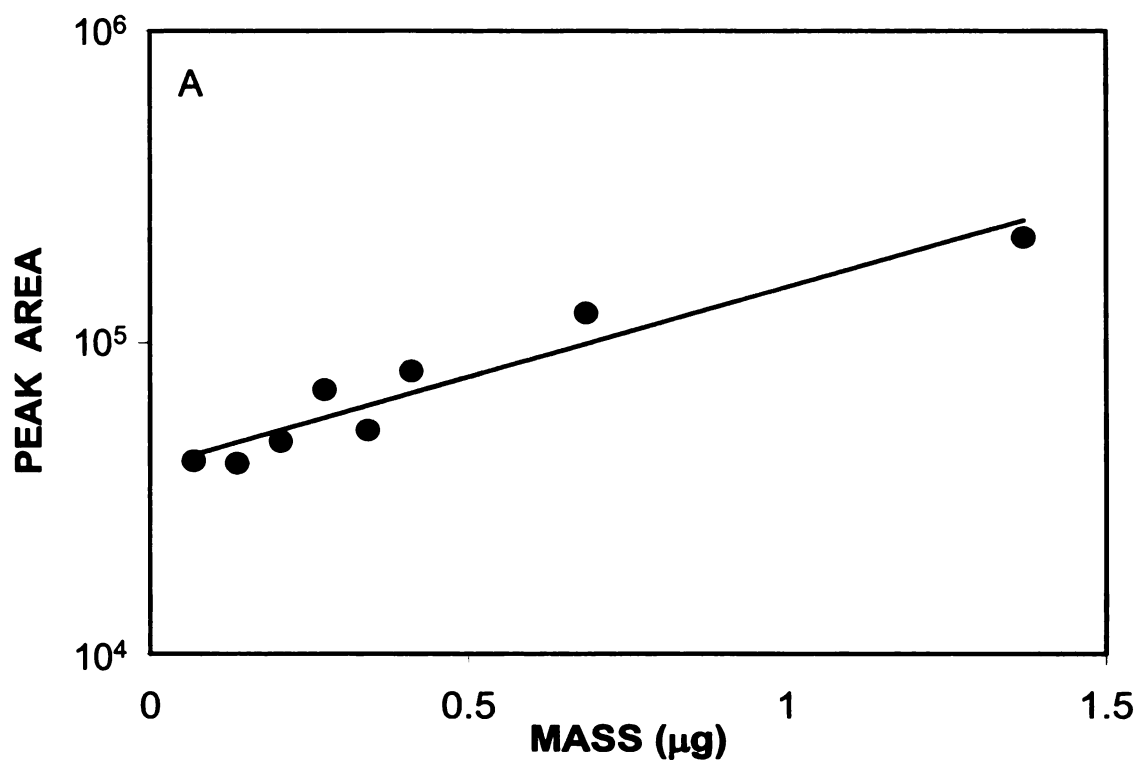


**Figure 3.12.** Calibration curves for picric acid based on peak area using (A) the semi-logarithmic fit described in Equation 3.4 and (B) the logarithmic fit described in Equation 3.5.

degradation products, the logarithmic expression increased the quality of fit and linear range significantly, making it much more useful in the analysis of a sample of unknown concentration. The linear range for the semi-logarithmic fit was one order of magnitude, which was extended to 2 – 3 orders of magnitude by using the logarithmic fit. The regressions for all three explosives were greatly improved, although the quality of fit for tetryl was lower than those for TNT and picric acid. In fact, the logarithmic fit for picric acid had the greatest correlation coefficient of all of the nitrated compounds.

Detection limits were also calculated for each of the nitroaromatic explosives using both the semi-logarithmic (Table 3.4) and logarithmic fits (Table 3.5) of the peak height data. The semi-logarithmic fit was so poor that the calculated detection limit was negative and was therefore not meaningful. Detection limits for TNT and tetryl were in the low  $\mu\text{g}$  range, as observed for the degradation products and were comparable to densitometry.<sup>8,9</sup> Using the logarithmic fit, detection limits for all solutes were also in the low  $\mu\text{g}$  range.

### **3.7 Quantitation of Nitramine Explosives**

Calibration curves were calculated using Equations 3.4 and 3.5 and are shown in Figures 3.13 and 3.14 for RDX and HMX, respectively. Tables 3.4 and 3.5 summarize the correlation coefficients for the semi-logarithmic and logarithmic fits of the data, respectively. Again, because curves for peak height and area followed the same trend, only peak area curves are shown.

For RDX and HMX, the logarithmic expression over the entire concentration range (Equation 3.5) was a better fit to the data than the semi-

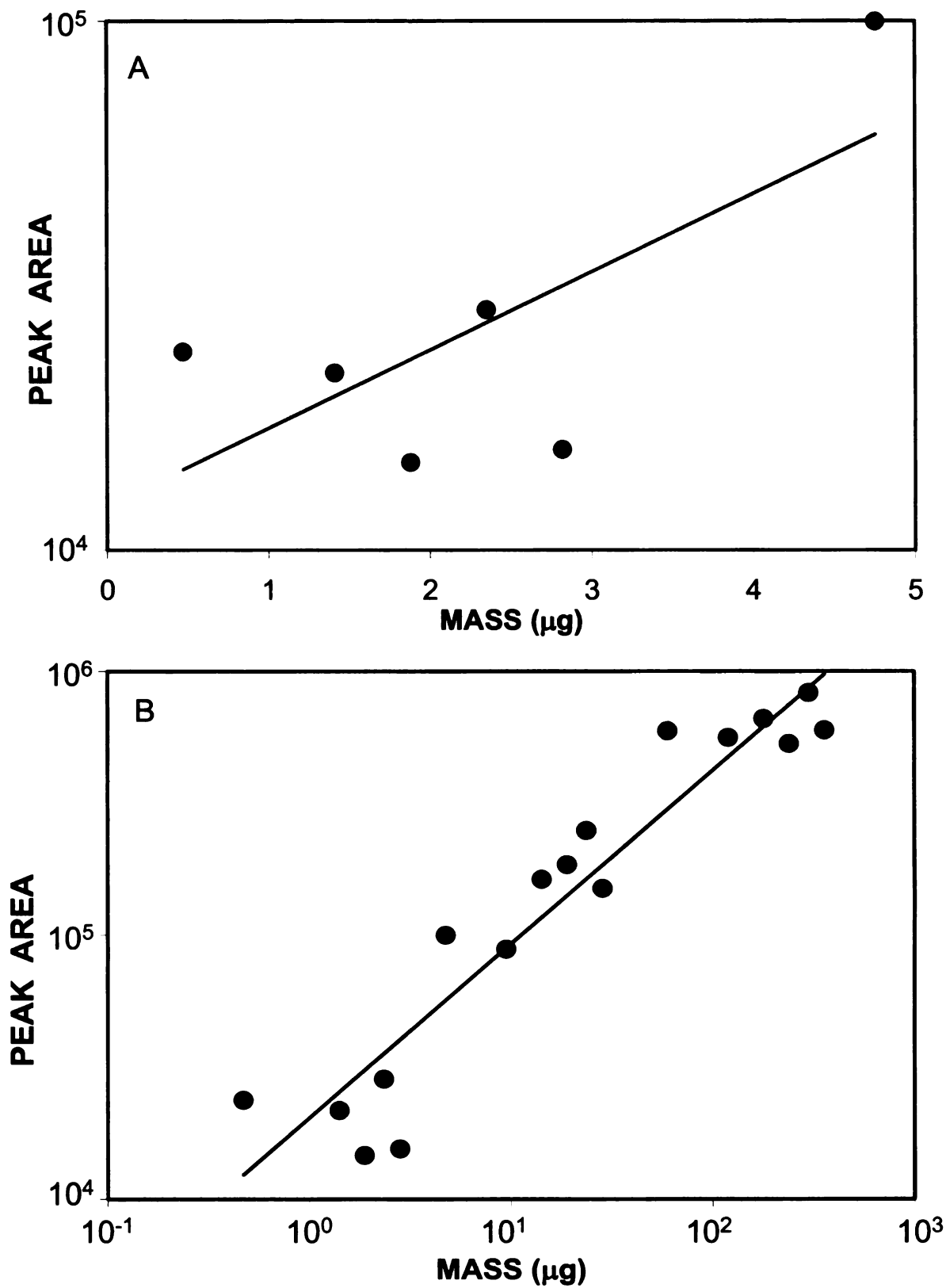


**Figure 3.13.** Calibration curves for RDX based on peak area using (A) the semi-logarithmic fit described in Equation 3.4 and (B) the logarithmic fit described in Equation 3.5.

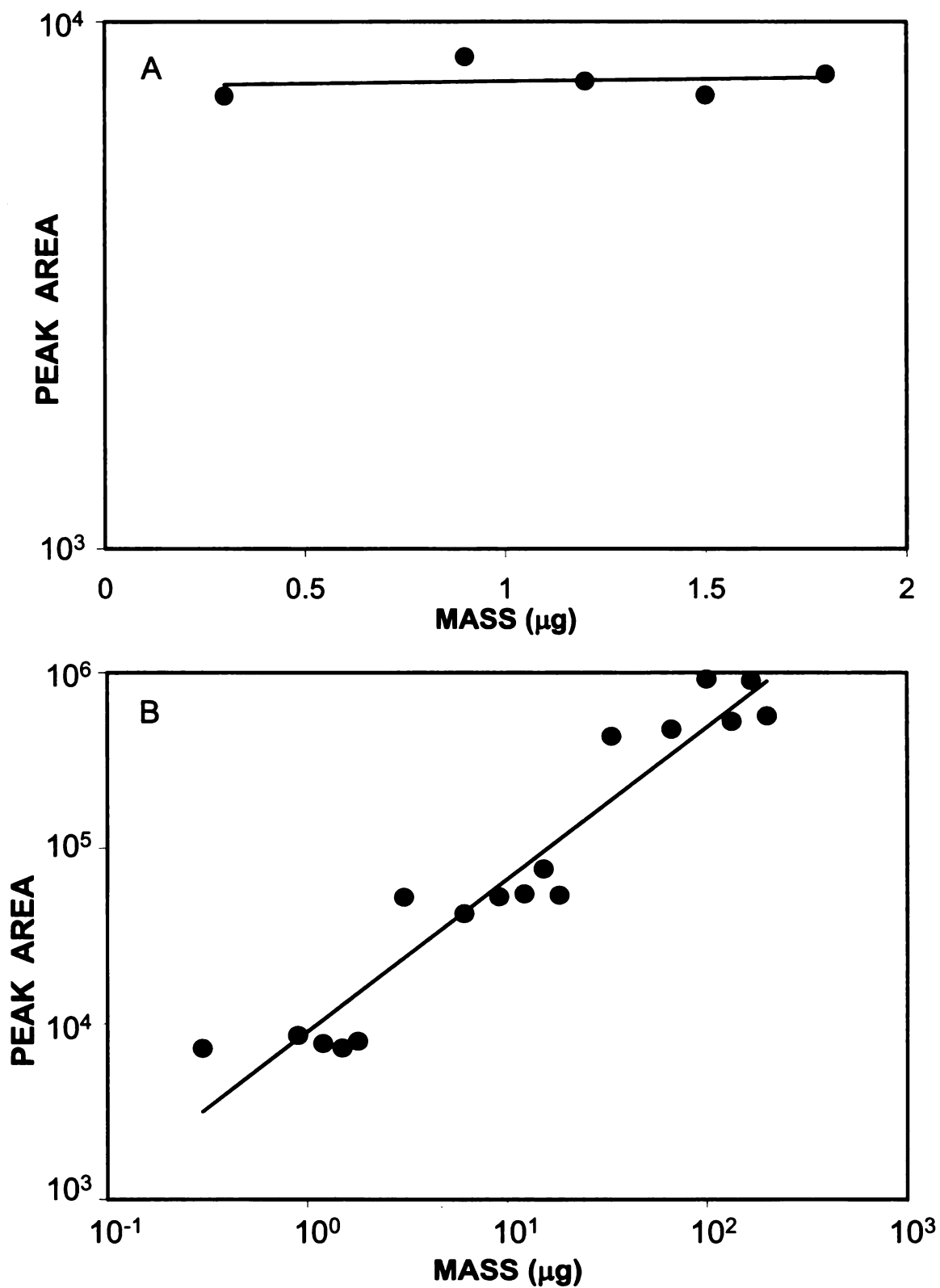


**Figure 3.14.** Calibration curves for HMX based on peak area using (A) the semi-logarithmic fit described in Equation 3.4 and (B) the logarithmic fit described in Equation 3.5.

logarithmic expression at low concentration (Equation 3.4), as seen from the correlation coefficients (Tables 3.4 and 3.5). For the semi-logarithmic expression, correlation coefficients varied from 0.03 to 0.5, and the poor qualities of fit were obvious from Figures 3.13A and 3.14A. Correlation coefficients for the logarithmic expression were improved to 0.87-0.92, although the fits were still quite poor (Figures 3.13B and 3.14B). Although the correlations were poor, use of the logarithmic expression increased the linear range to two orders of magnitude, making it more useful in the analysis of a sample of unknown concentration. The correlation coefficients for the nitramine explosives were more comparable to those for nitroaromatic explosives, and were less than those for many of the degradation products.

Detection limits were also calculated for RDX and HMX using both the semi-logarithmic (Table 3.4) and logarithmic (Table 3.5) fits of peak height data. The semi-logarithmic fit was so poor for HMX that the detection limit was negative and was therefore not meaningful. The detection limit for RDX using the semi-logarithmic fit was determined to be 5  $\mu\text{g}$ , which was the highest concentration used in the semi-logarithmic fit. Detection limits calculated using the logarithmic expression were also in the low  $\mu\text{g}$  range, which were comparable to those for nitroaromatic compounds and literature values for densitometry.<sup>1</sup>

### **3.8 Quantitation of Nitrate Ester Explosives**

Calibration curves were calculated using Equations 3.4 and 3.5 and are shown in Figures 3.15 and 3.16 for NG and PETN, respectively. Again, because curves for peak height and area followed the same trend, only peak area curves

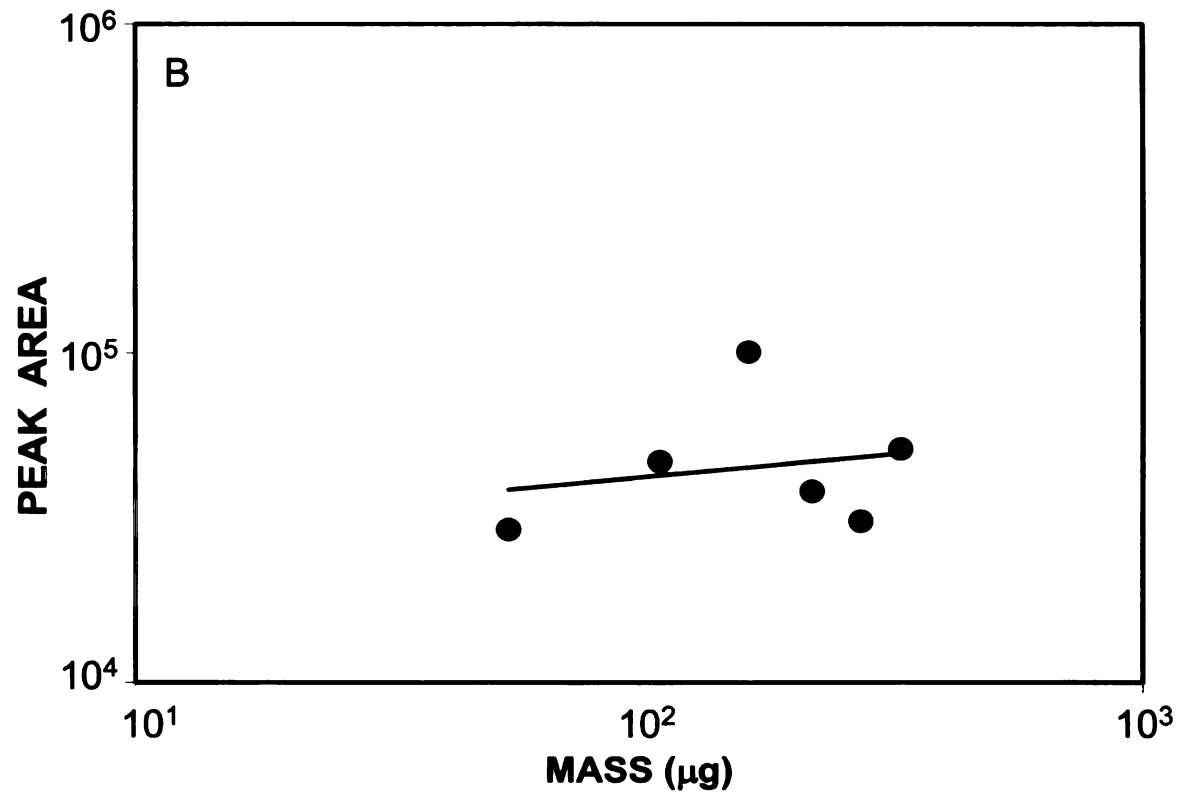
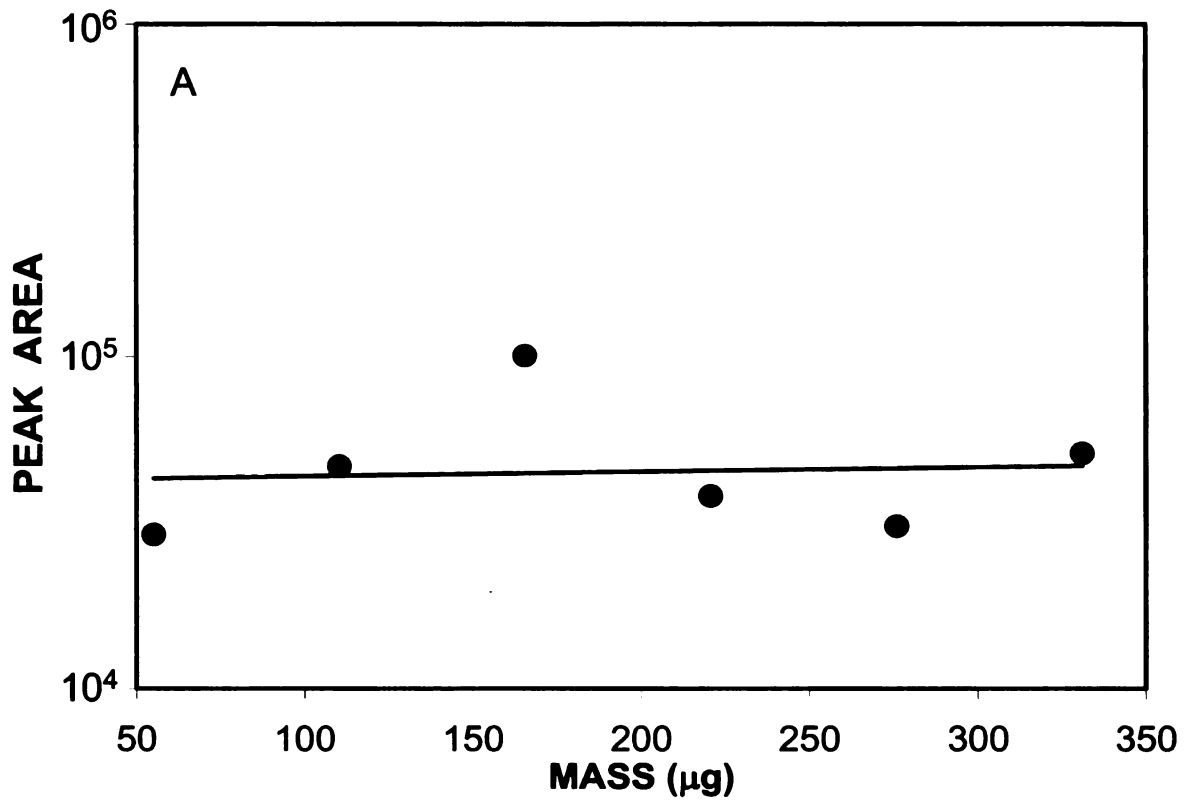


**Figure 3.15.** Calibration curves for NG based on peak area using (A) the semi-logarithmic fit described in Equation 3.4 and (B) the logarithmic fit described in Equation 3.5.

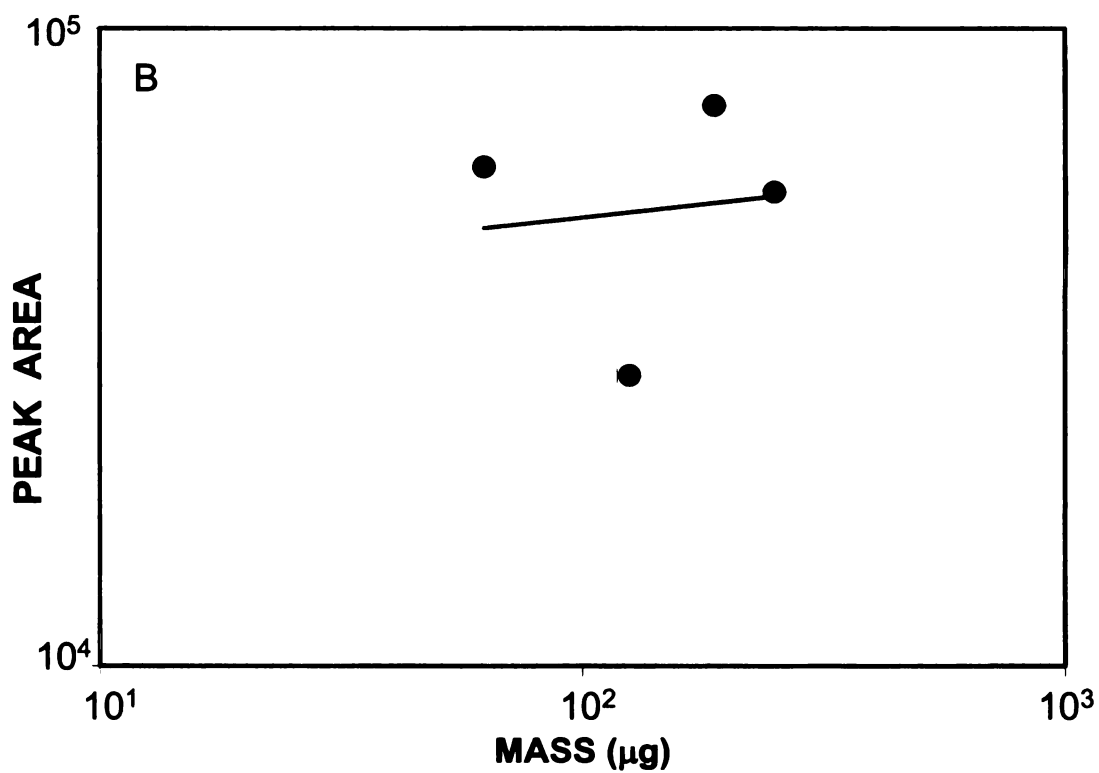
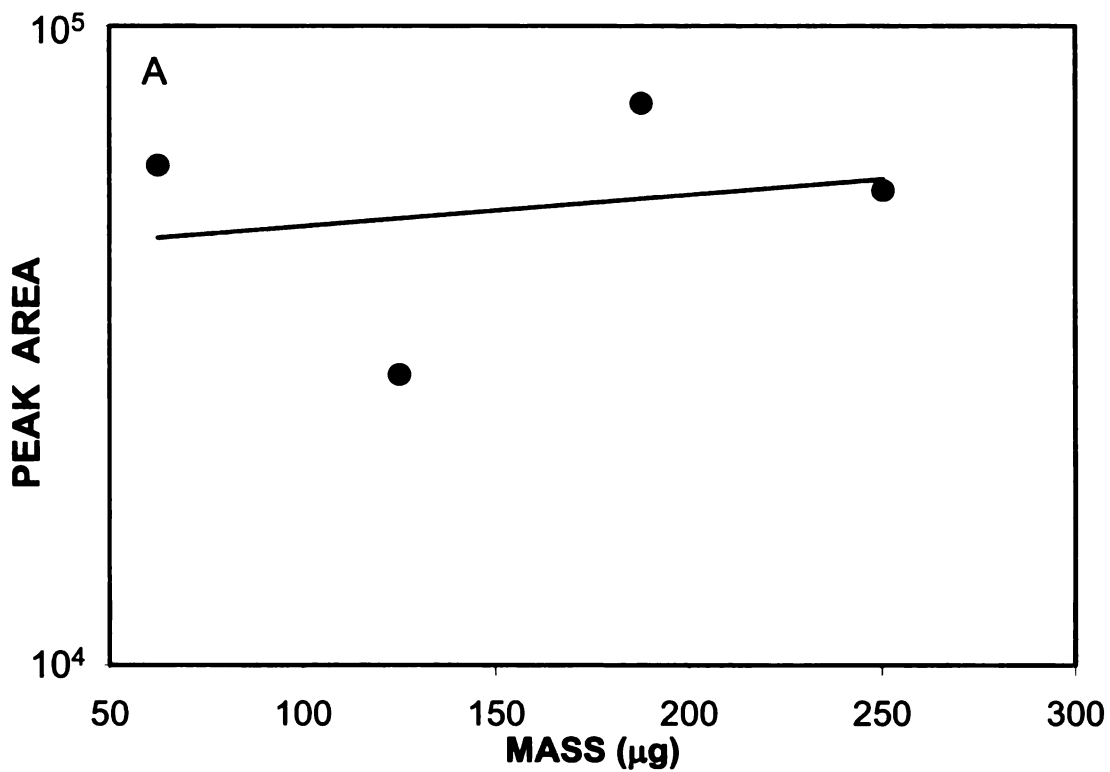


**Figure 3.16.** Calibration curves for PETN based on peak area using (A) the semi-logarithmic fit described in Equation 3.4 and (B) the logarithmic fit described in Equation 3.5.

are shown. Tables 3.4 and 3.5 summarize the correlation coefficients for the semi-logarithmic and logarithmic fits of the data, respectively. For both expressions, the quality of fit was very poor, with correlation coefficients less than 0.05. The low correlation coefficients led to difficulties in estimation of linear ranges and detection limits. Because NG and PETN have limited absorbance at 254 nm, higher concentrations were necessary to obtain a measurable quenching signal. For the nitrate ester explosives, masses below 50  $\mu\text{g}$  were undetectable, and masses above 250  $\mu\text{g}$  had asymmetric zones, making determination of  $R_f$  values difficult and narrowing the workable concentration range. The need for higher concentrations also led to nonlinear behavior of the adsorption isotherm (vide infra), resulting in a decreased upper limit of the concentration range relative to the other nitrated explosives. In addition, the estimated linear ranges and detection limits for NG and PETN were at significantly larger masses than those obtained for the other nitrated explosives (Tables 3.4 and 3.5).

### **3.9 Quantitation of an Unknown Explosive Sample**

Using the imaging system described here, quantitation of two unknown explosive samples was achieved. For each blind sample, a known quantity of explosive compounds was applied by a volunteer as described in Chapter 2 (Section 2.8). After development in the solvent systems discussed previously, the TLC plates were imaged using the CCD camera. A background plate was also imaged at the same time. The images were manipulated as discussed in Section 3.2 and the peak areas and peak heights were used to calculate the

mass of sample by using previously acquired calibration curves and Equations 3.4 and 3.5 (Table 3.6). Using the semi-logarithmic relationship (Equation 3.4), the calculated masses were less than the actual masses for all solutes except picric acid. For 2,6-DNT, TNT, and picric acid, the mass in the unknown was outside the linear range for this relationship (Tables 3.4 and 3.5), so the discrepancies were not surprising. The calculated mass of picric acid was within error of the actual mass. The calculated masses for 4-am-DNT and RDX were within a factor of two of the actual masses. For 2,6-DNT and TNT, however, logarithmic fit (Equation 3.5) was much more accurate, again with calculated masses within a factor of two of the actual mass.

The error in each determined value was determined by the method of propagation of error, not by replicate measurements. The error on each calculated mass was large, greater than 10% for most of the compounds. For some solutes, the error was nearly 50%. Although replicate measurements may provide a more accurate mass for an unknown sample, the time required would be too great for field analysis. Despite the large error, the values were within a factor of two of the true value using previously acquired calibration curves. With frequent calibration or internal calibration using standards of known concentration, however, the accuracy of the quantitation would be greatly improved. Therefore, the most practical procedure would be to use this imaging method to estimate the concentration of an unknown explosive, but to use a more sophisticated laboratory method or simultaneous calibration standards to determine the accurate quantity.

**Table 3.6.** Analysis of unknown explosive samples.

Solute	Actual Mass ( $\mu\text{g}$ )	Calculated Mass ( $\mu\text{g}$ )			
		Semi-logarithmic Fit <sup>a</sup>	Peak Height	Logarithmic Fit <sup>b</sup>	Peak Area
2,6-DNT	38.6	10 $\pm$ 5	70 $\pm$ 20	11 $\pm$ 5	80 $\pm$ 20
4-am-DNT	2.65	1.5 $\pm$ 0.3	0.87 $\pm$ 0.08	1.4 $\pm$ 0.2	0.81 $\pm$ 0.04
Picric acid	4.93	7 $\pm$ 2	21 $\pm$ 3	7 $\pm$ 2	29 $\pm$ 3
RDX	3.33	1.3 $\pm$ 0.2	2.6 $\pm$ 0.1	1.5 $\pm$ 0.2	2.65 $\pm$ 0.09
TNT	11.4	6 $\pm$ 4	8 $\pm$ 1	5 $\pm$ 3	5.6 $\pm$ 0.6

<sup>a</sup> Calculated using Equation 3.4.

<sup>b</sup> Calculated using Equation 3.5.

### **3.10 Additional Observations**

As mentioned for NG and PETN, many of the solutes exhibited streaking on the TLC plate at high concentrations, analogous to a tailing peak shape often observed in liquid chromatography under similar conditions. At high mass, the linear region of the adsorption isotherm was likely exceeded, causing overloading of the adsorption sites of the stationary phase. Although the shape of the zones was irregular in these regions, the values measured for peak height and area remained in the linear region of the calibration curve. Hence, one advantage of this method was that even with large sample amounts, the linearity of the calibration curve was maintained and quantitation was possible.

The linearity and detection limits calculated in this study were at much greater concentrations than those cited in the literature. A high degree of linearity was observed by Simon<sup>1</sup> for concentrations 1 to 2 orders of magnitude lower than those used in this study, based on images obtained using a cooled, spectroscopic-grade CCD camera with reduced background noise. In this study, higher concentrations were necessary to visualize the solutes on the TLC plates using a standard digital camera. Although this method was less sensitive, use of an uncooled camera was more relevant to proposed field applications. For field applications, linearity and detection limits cannot be directly compared to those using more sophisticated laboratory equipment, but the detection limits determined in this study should be sufficient for preliminary screening.

### **3.11 Conclusions**

Quantitation of nitrated explosives and degradation products following TLC was accomplished by using images acquired with a computer-controlled CCD camera. The imaging system was optimized to provide the most reliable quantitative data. The peak height and area of the solute zone were correlated to the mass of solute deposited on the plate using both a semi-logarithmic and logarithmic relationship. The semi-logarithmic relationship was only valid at low solute concentrations, while the logarithmic relationship could describe the entire concentration range. In general, the logarithmic relationship provided the best fit to the data and therefore the most reliable quantitation. Explosives and degradation products were quantitated over three orders of magnitude with practical detection limits in the low microgram ( $\mu\text{g}$ ) range. For routine use in a forensic laboratory, this method is advantageous because no reagents are required and quantitation can be performed with a handheld UV lamp and a digital camera. Using this standard equipment, the calculated detection limits were comparable to more sophisticated quantitation techniques. The practical utility of this method was explored, and quantitation of the explosive content in two blind samples was achieved.

### 3.12 References

1. Simon, R. E.; Walton, L. K.; Liang, Y.; Denton, M. B. *Analyst* **2001**, *126*, 446-450.
2. Skoog, D. A.; Holler, F. J.; Nieman, T. A. *Principles of Instrumental Analysis*, 5th ed.; Saunders College Publishing: Philadelphia, 1998.
3. St. John, P. A.; McCarthy, W. J.; Winefordner, J. D. *Anal. Chem.* **1967**, *39*, 1495-1497.
4. Pearson, E. S.; Hartley, H. O., Eds. *The Biometrika Tables for Statisticians.*, 3rd ed.; Cambridge University Press: Cambridge, 1966.
5. Bladdek, J.; Miszczak, M.; Popiel, S. *Chem. Anal. (Warsaw)* **1995**, *40*, 723-729.
6. Goodpaster, J. V.; McGuffin, V. L. *Anal. Chem.* **2000**, *72*, 1072-1077.
7. McGuffin, V. L.; Goodpaster, J. V. In *Encyclopedia of environmental analysis and remediation.*; Meyers, R., Ed.; Wiley: New York, NY, 1998, pp 3815-3831.
8. Liu, Y.; Wei, W.; Wang, M.; Pu, Y.; Lin, L.; Zhang, J. *J. Planar Chromatogr.* **1991**, *4*, 146-149.
9. Gholamian, F.; Chaloosi, M.; Waquif-Husain, S.; Dehghani, H. *J. Planar Chromatogr.* **2001**, *14*, 296-299.

## **CHAPTER 4. CONCLUSIONS AND FUTURE DIRECTIONS**

This project has sought to improve the TLC separation and detection of nitrated explosives for infrequent cases involving local law enforcement and forensic scientists. Unlike cases of national security or on the front lines of international conflicts where sophisticated technologies are available and widely used, local cases are less frequent and must be solved with the same accuracy but with fewer resources. One of the most common preliminary screening techniques used in these situations is TLC with spray reagents, followed by determination by visual inspection.

The first improvement made to this technique was through the incorporation of less toxic solvents to reduce safety concerns while maintaining the inherent simplicity of TLC. Using the two mobile-phase systems described in this work, a two-step separation can be used to determine up to 12 nitrated explosives. After application of an unknown mixture, plate development in 88:12 hexane:THF will separate nitroaromatic and nitrate ester explosives. Nitramine explosives and picric acid will remain at the original location, as the hexane:THF mobile phase is not sufficiently strong to cause their migration. After identification of the nitroaromatic and nitrate ester explosives, a second development in 65:35 hexane:MEK will provide separation of the nitramine explosives and picric acid. The identification of these compounds is accomplished by visual inspection under a UV lamp, which allows comparison of retention factors in an unknown and standard sample. This method was successfully utilized in the identification of two unknown explosive samples. One

blind sample was found to contain 4-am-DNT and TNT and a second was found to contain 2,6-DNT, RDX, and picric acid. Future work could extend this method for use with other compounds not considered in this work, such as inorganic or peroxide explosives.

Improvements have also been made in the quantitation of nitrated explosives following TLC separation. Quantitation of nitrated explosives and degradation products following TLC was accomplished by using images acquired with a computer-controlled CCD camera. The imaging system was optimized to provide the most reliable quantitative data. The peak height and area of the solute zone were correlated to the mass of solute deposited on the plate using both a semi-logarithmic and a logarithmic relationship. The semi-logarithmic relationship was only valid at low solute concentrations, while the logarithmic relationship could describe the entire concentration range. In general, logarithmic relationship for peak area provided the best fit to the data and therefore the most reliable quantitation. Explosives and degradation products were quantitated over three orders of magnitude with practical detection limits in the low microgram range. For routine use in a forensic laboratory, this method is advantageous because no reagents are required and the quantitation can be performed with a handheld UV lamp and a digital camera. Using this standard equipment, detection limits were comparable to more sophisticated quantitation techniques such as densitometry. In addition, this method provides qualitative and quantitative information simultaneously, and the sample can be preserved on the TLC plate and extracted from the stationary phase for further analysis in its

original form. This quantitation method was utilized in the analysis of two unknown explosive samples. Quantitative determination of picric acid was successful, with the concentration determined accurately within experimental error. For four other compounds, this quantitation method estimated the concentrations to be within a factor of two of the actual concentrations. The utility of the method for estimating unknown sample concentrations has been demonstrated, and improved quantitation can be achieved through further laboratory analysis.

Future work on this project would involve design and implementation of a field analysis system to incorporate the separation and quantitation components. This system should be relatively inexpensive and contain all components required for complete analysis. Mobile phase mixtures could be prepared in sealed pouches that would be opened immediately prior to use. Pre-washed TLC plates could also be sealed and opened immediately prior to use. Additional investigations would be necessary to determine the optimal extraction conditions to be used for unknown samples. Two small development chambers (~20x15x5 cm) would allow complete, simultaneous analysis of 2 unknowns in less than 10 minutes. Following separation, the plates could be placed in a static holder under UV illumination for imaging by a digital camera. A computer program could be developed that would identify solute zones and measure  $R_f$  values. The program could also be used to store background images and calibration curves, select areas for pixel value summation, and calculate corrected intensities from images. Ideally, the program would also calculate peak heights and areas and

estimate concentrations from stored calibration curves for each solute. Incorporation of these tasks into a computer program removes some subjectivity of the technician or forensic scientist, and increases the objectivity of the analysis. The program could then provide a printout or sound an alarm to notify the technician of the presence of an explosive. This work, and the work that will follow, can provide a simple, non-hazardous, and cost-effective method for separation and quantitation of nitrated explosives for local law enforcement agencies and forensic laboratories.

MICHIGAN STATE UNIVERSITY



3 1293 02956